AD-A092 642 INSTITUTE FOR DEFENSE ANALYSES ARLINGTON VA F/G 13/2
ON THE APPLICABILITY OF TWO- AND ONE-DIMENSIONAL PARAMETERIZATI--ETC(U)
APR 80 H HIDALGO DOT-FA77WA-3965
UNCLASSIFIED IDA-P-1473 FAA/EE-80-13 NL

1 OF 1
AD
A092642

END
DATE
FILMED
1-81
DTIC

Report No. FAA-EE-80-13

12 B.S.

ON THE APPLICABILITY OF TWO- AND ONE-DIMENSIONAL PARAMETERIZATIONS OF ATMOSPHERIC TRACER TRANSPORTS TO PROGNOSTIC PHOTOCHEMICAL MODELS OF THE STRATOSPHERE

(Institute for Defense Analyses Paper P-1473)

Henry Hidalgo

April 1980

FINAL REPORT

Prepared for

HIGH ALTITUDE POLLUTION PROGRAM

U.S. DEPARTMENT OF TRANSPORTATION

FEDERAL AVIATION ADMINISTRATION

Office of Environment and Energy

Washington, DC 20591

Technical Report Documentation Page

1. Report No.: FAA-EE-80-13
2. Government Accession No.: AD-A092 842
3. Recipient's Catalog No.:
4. Title and Subtitle: On the Applicability of Two- and One-Dimensional Parameterizations of Atmospheric Tracer Transports to Prognostic Photochemical Models of the Stratosphere
5. Report Date: April 1980
6. Performing Organization Code:
7. Author(s): Henry Hidalgo
8. Performing Organization Report No.: IDA ~~Paper~~ P-1473
9. Performing Organization Name and Address: Institute for Defense Analyses, 400 Army-Navy Drive, Arlington, Va. 22202
10. Work Unit No. (TRAIS):
11. Contract or Grant No.: DOT-FA-77WA3965
12. Sponsoring Agency Name and Address: Department of Transportation, Federal Aviation Administration, Office of Environment and Energy, Washington, D.C. 20591
13. Type of Report and Period Covered: Final Report
14. Sponsoring Agency Code:
15. Supplementary Notes:

16. Abstract

This paper deals with the applicability of *empirical* parameterizations of *stratospheric* transports of chemically inert tracers to *predictive* or *prognostic* two- and one-dimensional photochemical models of the stratosphere and troposphere for the forecasting of anthropogenic effects on atmospheric ozone. The scope of this paper therefore includes: (1) a critical review and assessment of the prognostic utility of the parent Reed and German (1965) 2-D parameterization of stratospheric transports; (2) the implied assumption in representative subsidiary 2-D parameterizations used or for use in 2-D photochemical models; (3) use of GCM/tracer model data for a chemically inert tracer for the assessment of the prognostic utility of both 2-D and 1-D parameterizations of stratospheric transports; and (4) the outlook for the development of prognostic parameterizations of stratospheric transports.

17. Key Words: Atmospheric ozone, Anthropogenic Effects on Atmospheric Ozone, Stratospheric Transports of Tracers, SST Effects on Atmospheric Ozone, Photochemical Models of the Stratosphere and Troposphere, Wave Motions in the Stratosphere

18. Distribution Statement: Document is available to the public through the National Technical Information Service, Springfield, Virginia 22161

19. Security Classif. (of this report)	20. Security Classif. (of this page)	21. No. of Pages	22. Price
UNCLASSIFIED	UNCLASSIFIED	86	

Form DOT F 1700.7 (8-72) Reproduction of completed page authorized

ACKNOWLEDGMENTS

The author is indebted to Dr. Jerry D. Mahlman of the Geophysical Fluid Dynamics Laboratory (NOAA) for providing access to his numerical data and for many valuable discussions. He also acknowledges important communications with Dr. Edward F. Danielsen.

The author is grateful to Professors J.R. Holton, J. London, T. Matsuno, and Dr. C. Prabhakara for valuable review comments which helped to improve this paper.

The contents of this paper are, of course, the sole responsibility of the author and they should not be interpreted as being necessarily or fully endorsed by any of the above prominent meteorologists.

ABSTRACT

This paper deals with the applicability of *empirical* parameterizations of *stratospheric* transports of chemically inert tracers to *predictive* or *prognostic* two- and one-dimensional photochemical models of the stratosphere and troposphere for the forecasting of anthropogenic effects on atmospheric ozone. The scope of this paper therefore includes (1) a critical review and assessment of the prognostic utility of the parent Reed and German (1965) 2-D parameterization of stratospheric transports, (2) the implied assumption in representative subsidiary 2-D parameterizations used or for use in 2-D photochemical models, (3) use of GCM/tracer model data for a chemically inert tracer for the assessment of the prognostic utility of both 2-D and 1-D parameterizations of stratospheric transports, and (4) the outlook for the development of prognostic parameterizations of stratospheric transports.

CONTENTS

FIGURES

TABLES

SUMMARY

This paper deals with the applicability of *empirical* parameterizations of *stratospheric* transports of chemically inert tracers to *predictive* or *prognostic* two- and one-dimensional photochemical models of the stratosphere and troposphere for the forecasting of anthropogenic effects on atmospheric ozone. Because the prognostic value of available two-dimensional (2-D) parameterizations of stratospheric tracer transports depend on the viability of the *parent* Reed and German (1965) formulation, emphasis is placed here on basic limitations of such formulation. The prognostic viability of 1-D parameterizations of stratospheric tracer transports is evaluated from *comprehensive* 3-D GCM*/tracer model data for a chemically inert tracer as a function of tracer configuration in both the space and time domains as well as of tracer-source location.

General and specific results for both the parent and subsidiary 2-D parameterizations of stratospheric tracer transports are as follows:

- The 2-D Reed and German parameterization of tracer transports in the critical region of the lower stratosphere is based on the crucial assumption that the macroscale vertical and meridional eddy transports, driven by well-structured stratospheric wave motions, may be described by the same turbulent mixing mechanisms as in the troposphere. As a consequence of this assumption, there is a need for drastic physical reinterpretation of the parent Reed and German formulation of stratospheric eddy transports, a formulation that is based on an adaptation

*General circulation model.

of the Prandtl mixing-length hypothesis for microscale turbulence. Hence, the applicability of the subsidiary 2-D parameterizations in available photochemical models for the *forecasting* of anthropogenic ozone effects is open to question.

- Viable prognostic parameterizations of stratospheric eddy transports for 2-D photochemical models require, in addition to the foregoing reinterpretation of the physical nature of the eddy fluxes, drastic modifications of the parent Reed and German formulation in regard to (1) the calculation of the statistics of the zonal average of both the slopes of the mixing-length paths or surfaces ($\bar{\alpha}$) and their deviation from such average ($\bar{\alpha}^{*2}$), and (2) the basic characteristics of the eddy transport coefficients (K's) which (a) may not have the $K_{yz} = K_{zy}$ symmetry as derived from implicit assumptions in the parent formulation (Eqs. 7 to 10 vs Eqs. 15 to 19) and (b) are not independent of the zonal ($\bar{u}$) and meridional ($\bar{w}$, $\bar{v}$) circulations as assumed in such parent formulation.

- A *strict* interpretation of the Reed and German 2-D formulation of eddy transports leads to: (1) apparent undeterminability from vertical and meridional GCM wind data (Tables 5 through 7) of the basic $\bar{\alpha}^{*2}/\bar{\alpha}^2$ statistics of the slope (α) of mixing-length paths and (2) over-specification of two eddy transport equations (Eqs. 4, 5) for one unknown eddy transport coefficient (K_{yy}) as a consequence of the required equality of the K_{yz} and K_{zy} eddy transport coefficients (Eq. 9). This latter result is opposite to current practice of using an undetermined system of two eddy flux equations (4, 5) for determining three unknown eddy coefficients (K_{yy}, K_{yz}, and K_{zz}; with $K_{zy} = K_{yz}$).

- Since the 2-D parameterizations of tracer transports used or for use in current representative photochemical models (Tables 1 to 3) assume equality of the K_{yz} and K_{zy} coefficients in the stratosphere and ignore the dependence of such coefficients on the zonal and meridional circulations, they cannot therefore rely on the viability of the Reed and German formulation to justify their *prognostic* utilization. Moreover, it is found that they are based on implied assumptions of the basic $\bar{\alpha}^{*2}/\bar{\alpha}^2$ statistics that are (1) not always positive, even though they involve a ratio of quadratic terms (Table 4); (2) drastically different among themselves (Table 4) instead of remaining fixed by the (same) wind variability of the stratosphere (Eq. 6); and (3) inconsistent with the parent Reed and German formulation due to the apparent undeterminability (Eq. 14) of such statistics.

- Use of 3-D GCM/tracer model data for the evaluation of 2-D parameterizations of eddy transports, when they are based on the assumption that $\bar{\alpha}^{*2}/\bar{\alpha}^2 = 0$ everywhere in the lower stratosphere at middle and high latitudes (Table 1), indicate the following: (a) the eddy coefficients would have to become negative in some regions of the stratosphere (Tables 9 and 10), and (b) when aircraft emissions are introduced continuously in the lower stratosphere, the $\bar{\alpha}$ (or K_{yz}/K_{yy}) parameter would also have to change instead of remaining fixed by the wind variability (Table 8).

- The significant differences in the magnitude of the eddy transport coefficients, as given by available representative 2-D parameterizations of eddy transports in the lower stratosphere (e.g. Tables 2 vs 3), appear to stem from two factors: (1) use of different types of observed tracer data for the determination of such coefficients and (2) the fact that, as indicated by

GCM/tracer model data, the eddy transports of anthropogenic tracers depend on the time (age in years) and/or space (source location) configurations of the tracers in the stratosphere.

- Available preliminary results from a Lagrangian instead of Eulerian description of air parcel motions caused by a planetary wave in the stratosphere indicate the possibility for a prognostic 2-D formulation of eddy transports which would (1) have no need for the Reed and German constraint on an equality of the K_{yz} and K_{zy} eddy transport coefficients, and (2) relate the eddy transport coefficients to the period of oscillation of air parcels due to planetary waves, which, in turn, relates to the zonal circulation.

In regard to the *prognostic* applicability of empirical 1-D parameterizations of stratospheric transports in 1-D photochemical models, comprehensive 3-D GCM/tracer model data (Table 11) indicate the following:

- The magnitude of the 1-D transport coefficients in the critical region of the lower stratosphere can (1) become negative for SST emissions, a result that implies distortions of the K(z) profile and (2) depend on the tracer configuration in the stratosphere as given by the source location, source characteristics, and tracer age or years. Therefore, the empirical parameterizations of stratospheric transports used in 1-D photochemical models appear to lack physical basis for their *prognostic* utilization, since they are assumed to be always positive and independent of tracer configuration in the stratosphere.

Although the magnitudes of 1-D coefficients derived from 3-D GCM/tracer model data may be dependent on the vertical resolution of the model in the critical tropopause and lower

stratosphere regions, the trends established by extensive calculations of such a model during the last several years may not be ignored in the absence of worldwide observations of suitable tracers for an ensemble of many years. In fact, a promising avenue to derive more exact 1-D transport coefficients is to improve the vertical resolution of the GCM/tracer model instead of ever attempting to collect empirical data for a suitable tracer in the lower stratosphere over a worldwide space domain and for an ensemble of many years.

I. INTRODUCTION

A need to forecast long-term effects of high-altitude aircraft engine emissions (NO_x and H_2O) on atmospheric ozone as a function of altitude, latitude, and season has led to an interest in the development of predictive or prognostic two-dimensional (2-D) photochemical models of the stratosphere and troposphere (e.g. Hidalgo and Crutzen, 1977; and Widhopf, Glatt, and Kramer, 1977). A basic component of such models is the description of large-scale vertical and latitudinal or meridional transports of tracer mixing ratio for the determination of the 2-D distributions of relevant natural and anthropogenic chemical species. The development of prognostic 2-D photochemical models of the stratosphere and troposphere has then consisted in the generation of numerical solutions of time-dependent partial differential equations for the conservation of each of the involved chemical species with specified (Hidalgo, 1978): (1) vertical and meridional mean winds as well as eddy transport coefficients as a function of altitude, latitude, and month (season); (2) photolysis rates and short-wave solar radiation for the relevant photochemistry; (3) reaction rates for the involved chemical kinetics; (4) rate constants for the heterogeneous chemistry involving sinks of water-soluble chemical species in the lower troposphere; and (5) anthropogenic sources of chemical tracers as a function of atmospheric location and time (years). The computing scheme is completed by using for each of the chemical species initial conditions throughout the model atmosphere as well as appropriate boundary conditions at the earth's surface and stratopause.

Two main applications of 2-D photochemical models during the last several years have been (1) *diagnostic* calculations of the *prevailing* mixing ratio of relevant chemical species as a function of altitude, latitude, and season in the stratosphere and troposphere; and (2) prognostic forecasts of long-term, global-scale ozone effects from specified future aircraft emissions as a function of altitude and latitude. Since effective regulations designed to prevent predicted long-term adverse ozone effects on a global scale would require international participation, the scrutiny and documentation of each of the above foundations of 2-D photochemical models must be such as to promote international credibility of their predictions concerning any anthropogenic threat to atmospheric ozone.

The objective of this paper is to examine the description of the large-scale vertical and meridional transports of chemical species as used or intended for use in current representative 2-D photochemical models of the stratosphere and troposphere. Furthermore, since such descriptions of tracer transports are based on extensions or interpretations of the parent Reed and German (1965) formulation for chemically inert tracers in the stratosphere, emphasis must be placed here on this parent formulation. Considerations of interest are then on the following:

- Need to distinguish between the *diagnostic* use of empirical parameterizations of stratospheric transports and the *prognostic* use of such empiricism for the forecasting of future anthropogenic effects on ozone.
- Need to compare on a common basis different, representative 2-D parameterizations of tracer transports used or for use in 2-D photochemical models.
- Need to bring out any basic limitation in the pioneering Reed and German formulation, which was devised

over a decade ago for diagnostic calculations of chemically inert tracers in the stratosphere and in the absence of current 3-D general circulation model (GCM) data for unmeasurably small large-scale vertical transports in the stratosphere. An indirect tribute to the difficulty of such a pioneering effort is the fact that there is not yet an adequate solution to the 2-D formulation of tracer transports in the stratosphere.

- Need to clarify past interpretations concerning basic concepts of the parent Reed and German formulation of tracer transports in the stratosphere.

Hence, the main scope of this paper includes the following: (1) review of the Reed and German parameterization of the transports of chemically inert tracers in the stratosphere; (2) implied assumptions in the parameterizations of tracer transports in current representative 2-D photochemical models; (3) apparent undeterminability of fundamental statistics in the Reed and German parameterization; (4) constraints in basic Reed and German results that are carried over to the 2-D parameterizations in photochemical models; (5) past interpretations of basic Reed and German results; and (6) outlook for future progress in the development of prognostic 2-D formulations of tracer transports. Finally, because of the widespread use of 1-D parameterizations of atmospheric transports in the more versatile 1-D photochemical models, this paper includes considerations of the limitations of 1-D empiricism for the prognostic representation of atmospheric transports.

II. REVIEW OF REED AND GERMAN FORMULATION

The basic aim of 2-D parameterizations of stratospheric transports in photochemical models is to describe the zonal-monthly (seasonal) statistical averages of vertical and meridional transports of chemical species in stratospheres that are characterized by either the absence or presence of aircraft engine emissions of NO_x (NO, NO_2) and H_2O. Because of the interest in monthly (seasonal) anthropogenic ozone effects, the primary concern is with the statistics of tracer transports by large-scale wave motions. Two basic assumptions used in representative 2-D photochemical models of the stratosphere and troposphere are (1) decoupling of the chemistry from the temperature and wind fields, and (2) use of the Reed and German adaptation of the Prandtl (1925) mixing-length hypothesis to the macroscale eddy transports in the stratosphere. Each of these assumptions is described below.

A. DECOUPLING OF CHEMISTRY FROM THE TEMPERATURE AND WIND FIELDS

The first basic assumption in representative 2-D photochemical models of the stratosphere and troposphere is that the conservation equations for chemical species are decoupled from the primitive equations of the general circulation (e.g. Lorenz, 1967). Since the latter equations can be used to obtain estimators of the monthly (seasonal) statistics of the temperature and wind fields in the stratosphere, an implicit assumption in the 2-D photochemical models is that the anthropogenic redistributions of radiatively and chemically active tracers (e.g. ozone) will not produce first-order effects on the monthly statistics of the temperature and winds in the stratosphere. A

consequence of such decoupling is that such 2-D photochemical models cannot then take into account feedback effects of the calculated ozone redistributions on the original statistics of the background temperature and wind fields. Obviously, the validity of the decoupling of the chemistry from the temperature and wind fields would become open to question as the magnitude of the calculated changes in ozone by all anthropogenic effects become increasingly large.

The interactions of the photochemistry and chemical kinetics with the temperature and wind fields are given by a set of continuity equations for the chemical species in an oxygen-hydrogen-nitrogen-chlorine atmosphere, i.e., by

$$\frac{dR_i}{dt} = P_i - L_i \qquad (1)$$

where R_i is the mixing ratio for any ith of N given chemical species, t the time and P_i as well as L_i the corresponding production (including anthropogenic sources) and loss (or sink) chemical mechanisms.* The left side of Eq. (1) contains the influence of motions as identifiable by expanding the total derivative dR_i/dt.

The 2-D continuity equations for the conservation of chemical species are obtained by (1) taking the zonal-monthly statistical average of Eq. (1) for an ensemble of many years and (2) splitting the transports of mixing ratio into those by the mean winds and those by wave or eddy motions. For the case of chemically inert tracers, as in the Reed and German formulation, $P_i = L_i = 0$, $R_i = R$ and Eq. (1) simplifies to $dR/dt = 0$. In spherical

*The terms P_i and L_i in Eq. (1) have absorbed the air number density n as obtained from use of the continuity equation for both the ith chemical species (n_i) and air (n), together with $R_i = n_i/n$.

coordinates, the zonal-monthly statistical average of $d\bar{R}/dt$ becomes as in the Reed and German Eq. (2), i.e.,

$$\frac{\partial \bar{R}}{\partial t} = - \bar{V} \cdot \nabla \bar{R} - \frac{1}{\rho} \frac{\partial}{\partial z} \rho \overline{w^* R^*} - \frac{1}{\rho a \cos\theta} \frac{\partial}{\partial \theta} \rho \cos\theta \overline{v^* R^*} , \quad (2)$$

where $\bar{V}$ is the 2-D wind vector, ∇ the corresponding gradient vector for the mixing ratio, ρ the air density, w and v the upward and poleward winds, a is the mean radius of the earth, z the altitude, and θ the latitude. The Reed and German notation $(\bar{\ })$ denotes the estimators for the zonal-monthly ensemble average of ( ), whereas $(\ )^*$ is the deviation of ( ) from such average; i.e. $(\ )^* \equiv (\ ) - (\bar{\ })$. The right-hand side of Eq. (2) exhibits the roles of the transports of mixing ratio by (1) the meridional circulation ($\bar{V} \cdot \nabla \bar{R}$) or average vertical and meridional winds, (2) the vertical eddy motions (2nd term) and (3) the meridional eddy motions (remaining term).

B. ADAPTATION OF MIXING LENGTH HYPOTHESIS TO THE STRATOSPHERE

The numerical solution of the continuity equation (2) for a chemically inert tracer requires elimination of the eddy transport terms through their correlations with the vertical and meridional components of the gradient vector $\nabla \bar{R}$. For this purpose, the 2-D Reed and German representation of eddy transports adapts the Prandtl mixing-length hypothesis for turbulent transports of momentum in microscale flow to the macroscale transport by wave motions of chemically inert tracers in the stratosphere. As a consequence of this assumption, the Reed and German formulation carries over to the stratosphere the implicit assumptions that (a) the eddy tracer transports in Eq. (2) are independent of both the zonal and meridional circulations, when in fact they are intimately related (e.g. Hunt and Manabe, 1968; Holton, 1975); and (b) the eddy transports can then be correlated with gradients of mixing ratio, as in the Prandtl

mixing length hypothesis. Thus, if χ denotes a dependent variable such as potential temperature or ozone, a direct application of the Prandtl mixing length hypothesis would give $\overline{v^*\chi^*} = - K_y \, \partial\bar{\chi}/\partial y$; where $y = a\theta$ is taken as positive ($\Delta y > 0$) in the poleward direction. However, a basic difficulty then was that for a poleward eddy flux (i.e. $\overline{v^*\chi^*} > 0$), with $K_y > 0$, then $\partial\bar{\chi}/\partial y < 0$; i.e., the poleward eddy flux had to take place always in a downgradient direction from high to low values of $\bar{\chi}$ in opposition to observed countergradient eddy fluxes of, for example, ozone ($\overline{v^*O_3^*}$) or heat ($\overline{v^*T^*}$). Hence, in order to adapt the Prandtl mixing length hypothesis to countergradient eddy fluxes from low to high values of $\bar{\chi}$, it was postulated that the slope (α) of mixing length paths or surfaces would have to be larger than the slope (β) of the tracer isopleths $\bar{\chi}$ or isentropes when $\bar{\chi}$ represents the potential temperature. This concept is illustrated in Fig. 1, as given by Reed and German. The basic results of this 2-D formulation of the eddy transports are then as follows:

$$\chi^* = - \vec{\ell}\cdot\nabla\chi = - (\ell_y \frac{\partial\bar{\chi}}{\partial y} + \ell_z \frac{\partial\bar{\chi}}{\partial z}) \qquad (3)$$

where $\vec{\ell}$ is the mixing length vector ($\ell \sim 100$ km) with horizontal and vertical components ℓ_y and ℓ_z. When χ represents mixing ratio in Eq. (3), the desired correlations of the horizontal and vertical eddy fluxes in Eq. (2) with the components of $\nabla\bar{R}$ are given by

$$\overline{v^*R^*} = - (K_{yy} \frac{\partial\bar{R}}{\partial y} + K_{yz} \frac{\partial\bar{R}}{\partial z}) \quad , \qquad (4)$$

$$\overline{w^*R^*} = - (K_{zy} \frac{\partial\bar{R}}{\partial y} + K_{zz} \frac{\partial\bar{R}}{\partial z}) \quad , \qquad (5)$$

where $K_{yy} \equiv \overline{v^*\ell_y}$, $K_{yz} \equiv \overline{v^*\ell_z}$; $K_{zy} \equiv \overline{w^*\ell_y}$ and $K_{zz} \equiv \overline{w^*\ell_z}$. Using the fact that $\bar{\alpha} \simeq 10^{-4}$ and that the wind $\bar{V}$ is along the mixing length direction:

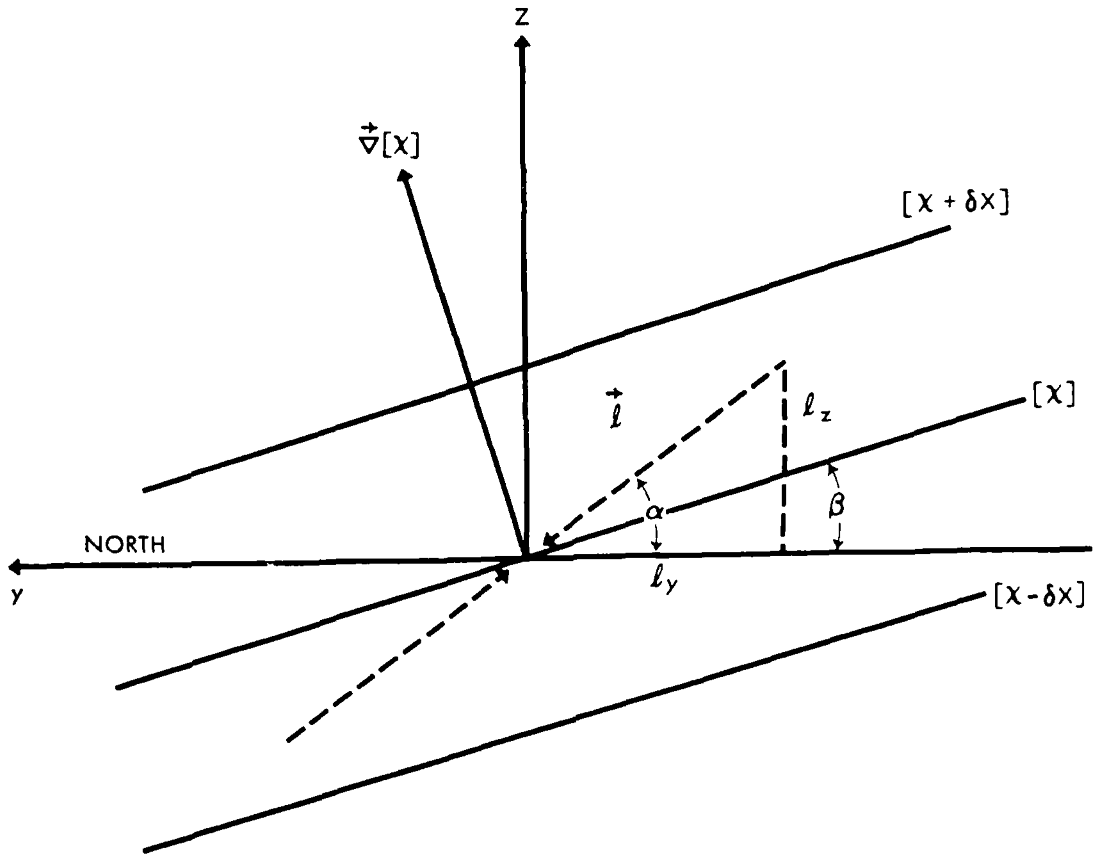

S-18-78-3

FIGURE 1. Schematic representation of the slope (α) of the mixing length path necessary for countergradient eddy fluxes in the Prandtl mixing length hypothesis, as given by Reed and German (1965). The eddy flux is countergradient here because both $\partial\bar{\chi}/\partial y$ and $\overline{v^*\chi^*}$ are positive. The former condition takes place because $\Delta\chi > 0$ when $\Delta y > 0$, and the latter because the eddy flux is poleward; a condition that can be visualized by letting χ represent the potential temperature. The dashed arrows then indicate the mixing at the origin of northward moving air parcels that are warmer than ambient with southward moving air parcels that are colder than ambient. Note that the countergradient eddy flux of heat $\overline{v^*T^*}$ is poleward whenever $\alpha > \beta$. Similar arguments apply when χ represents ozone to yield a countergradient flux characterized by $\partial\bar{O}_3/\partial y > 0$ and $\overline{v^*O_3^*} > 0$.

$$\begin{aligned} v^* &= V \cos\alpha \simeq V \\ w^* &= V \sin\alpha \simeq V\alpha \\ \ell_y &= \ell \cos\alpha \simeq \ell \\ \ell_z &= \ell \sin\alpha \simeq \ell\alpha \end{aligned} \qquad (6)$$

With Eqs. (6), the eddy coefficients K_{yy}, K_{yz}, K_{zy}, and K_{zz} can be expressed as follows:

$$K_{yy} = \overline{v^*\ell_y} = \overline{V\ell \cos^2\alpha} \simeq \overline{V\ell} \simeq K \qquad (7)$$

$$K_{yz} = \overline{v^*\ell_z} = \overline{V\ell \sin\alpha\cos\alpha} \simeq \overline{V\ell\alpha} \simeq \bar{\alpha} K \qquad (8)$$

$$K_{zy} = \overline{w^*\ell_y} = \overline{V\ell \sin\alpha\cos\alpha} \simeq \overline{V\ell\alpha} \simeq K_{yz} \qquad (9)$$

$$K_{zz} = \overline{w^*\ell_z} = \overline{V\ell \sin^2\alpha} \simeq \overline{V\ell\alpha^2} \simeq (\bar{\alpha}^2 + \overline{\alpha^{*2}})\, K \qquad (10)$$

where *it is assumed that* α *and* α^* *are independent of* V *and* ℓ, i.e., that they do not depend on the wind speed or the length of the mixing path. Substitution of Eqs. (7) through (10) into (4) and (5), using $\bar{\beta} \simeq \tan \bar{\beta} = -(\partial\bar{R}/\partial y)/(\partial\bar{R}/\partial z)$, alternative expressions for the eddy fluxes are given by

$$\overline{v^*R^*} = -K_{yy}\left(1 - \frac{\bar{\alpha}}{\bar{\beta}}\right)\frac{\partial\bar{R}}{\partial y} \quad , \qquad (11)$$

$$\overline{w^*R^*} = -K_{zz}\left(1 - \frac{\bar{\alpha}\ \bar{\beta}}{\bar{\alpha}^2 + \overline{\alpha^{*2}}}\right)\frac{\partial\bar{R}}{\partial z} \qquad (12)$$

Equation (11) indicates that (a) when $\bar{\alpha}/\bar{\beta} = 0$, the horizontal eddy flux becomes downgradient as in the Prandtl formulation for the microscale eddy transport of momentum; (b) when $\bar{\alpha}/\bar{\beta} = 1$, the horizontal eddy flux vanishes; and (c) when $\bar{\alpha}/\bar{\beta} > 1$, the horizontal flux becomes countergradient. Similar consideration can be made to the vertical eddy flux as given by Eq. (12).

III. PARAMETERIZATION OF EDDY TRANSPORTS FOR 2-D PHOTOCHEMICAL MODELS

The continuity equations in representative 2-D photochemical models are as Eq. (2), except that R must be replaced by R_i and the right-hand side must incorporate the $\bar{P}_i$ and $\bar{L}_i$ terms. The use of Eqs. (4) and (5) for each ith chemical tracer allows elimination of the eddy terms in these equations, which become differential equations for the mixing ratio of each tracer with specified average meridional winds and eddy transport coefficients. A fundamental approach in 2-D photochemical models then consists in (1) assuming that the eddy transport coefficients are independent of the chemical tracer, i.e., that they depend only on altitude, latitude, and month for a specified meridional circulation and (2) establishing the magnitude of the eddy transport coefficients from observations of distributions of natural (i.e. ozone, water vapor) and/or anthropogenic (i.e. radioactive debris from past nuclear explosions) tracers in the lower stratosphere. The parameterizations of eddy transports have then been reduced to the use of two eddy tracer flux equations (4, 5) for three unknown eddy transport coefficients (K_{yy}, K_{yz}, K_{zz}, i.e. with $K_{zy} = K_{yz}$) at given stratospheric meridional locations and month (season). This procedure has therefore required the use of additional constraints so as to resolve the undetermined foregoing system.

Three representative 2-D parameterizations of eddy transports utilizing nearly the same meridional circulation (i.e. Louis, 1974) are: (1) that in the Crutzen photochemical model (Hidalgo and Crutzen, 1977), (2) that in the Widhopf, Glatt, and Kramer (1977) model and (3) that given by Danielsen and

Louis (1975). The Crutzen parameterization of eddy transports utilized Eqs. (7) through (10), together with continuity equations for ozone and water in the presssure instead of the altitude coordinate as it is done in the other two parameterizations. The Widhopf et al. parameterization utilized Eqs. (4), (5), and (9), together with the continuity Eq. (2) for chemically inert tracers and (a) extrapolations to the stratosphere (by Luther, 1973) of the Oört and Rasmusson (1971) data for eddy transports of heat in the upper troposphere at latitudes $\theta \leq 50°$ N and (b) use of rather crude observations of the meridional distributions of mixing ratio for anthropogenic chemically inert radioactive tracers. The Danielsen and Louis parameterizations utilized Eqs. (4), (5), and (9), together with Eq. (2) for ozone in the lower stratosphere on the assumption that ozone could be considered there to be a chemically inert tracer; however, instead of using the continuity equation for water vapor in the stratosphere, as in the Crutzen parameterization, the Danielsen and Louis approach had to use constraints that would insure tropospheric ozone fluxes that were compatible with the ozone destruction at the ground.

Tables 1 through 3 (Hidalgo, 1978) illustrate the magnitude of the eddy transport coefficients K_{yy}, $\bar{\alpha}$ (or K_{yz}/K_{yy}), and K_{zz} from the foregoing parameterizations at critical altitudes for the exchange of anthropogenic tracers between the lower stratosphere and upper troposphere. Because of the significant differences in the magnitudes of these eddy coefficients, it is of interest to (1) contrast the direct use of Eq. (10) with $\bar{\alpha}^{*2} = 0$ in the Crutzen parameterization (Crutzen, 1980) as it is not done in the other two, and (2) emphasize the general dependence of eddy tracer transports on both the space and time (years) distributions of anthropogenic (i.e. radioactive) tracers in the stratosphere (Mahlman and Moxim, 1978; Hidalgo, 1978), i.e., the use of the eddy flux equations (4) and (5) with Eq. (9) tends to make the magnitude of the eddy coefficients dependent on the space and time (age) distributions of particular tracers in the lower stratosphere (Danielsen and Louis, 1975).

TABLE 1. SAMPLE EDDY PARAMETERS FOR CRUTZEN MODEL DURING SUMMER AND WINTER IN NORTHERN HEMISPHERE* (Source: Hidalgo and Crutzen, 1977)

Altitude (km)	Summer, Latitude (deg.)					Winter, Latitude (deg.)				
	80°N	60°N	40°N	20°N	0°N	80°N	60°N	40°N	20°N	0°N
	Eddy Transport Coefficient K_{yy}, (10^{10} cm^2/sec)									
19.8	1.44	1.12	0.80	0.43	0.30	4.40	4.40	3.80	1.18	0.31
18.0	1.44	1.12	0.80	0.47	0.36	4.40	4.40	3.80	1.22	0.37
16.3	1.44	1.12	0.80	0.54	0.45	4.40	4.40	3.80	1.29	0.45
14.5	1.44	1.12	0.91	0.59	0.48	4.40	4.43	4.52	1.46	0.48
12.7	1.44	1.28	1.13	0.64	0.48	4.48	5.42	5.65	1.72	0.48
10.8	1.66	1.61	1.28	0.68	0.48	5.46	6.82	6.08	1.88	0.48
	Slope of Mean Diffusion Axis, $\bar{\alpha}$ (10^{-4})									
19.8	-7.42	-12.14	-13.96	-5.00	-0.30	-5.03	- 9.24	-12.15	-4.29	-0.27
18.0	-7.85	-12.74	-14.71	-1.28	-0.25	-5.85	-10.24	-12.96	-0.43	-0.24
16.3	-8.30	-13.22	-12.40	-0.40	-0.19	-6.66	-11.14	- 9.74	0.41	-0.18
14.5	-8.34	-10.75	- 4.52	-0.18	-0.17	-7.24	-11.21	- 0.21	-0.67	-0.08
12.7	-6.77	- 3.13	0.95	-0.82	-0.15	-6.85	- 8.29	2.57	0.04	-0.04
10.8	-1.84	1.17	1.09	-1.68	-0.09	-4.56	0.29	2.51	-0.67	-0.04
	Eddy Transport Coefficient, K_{zz}, (10^4 cm^2/sec)									
19.8	1.71	2.16	1.77	0.36	0.12	2.30	4.34	4.79	0.58	0.12
18.0	1.60	2.20	1.85	0.29	0.12	2.56	4.97	5.17	0.39	0.12
16.3	1.57	2.12	1.56	4.23	15.70	2.90	5.61	1.57	4.31	16.13
14.5	1.44	1.38	0.81	5.26	14.10	3.11	5.08	1.62	5.37	14.44
12.7	0.93	0.83	0.61	6.41	12.52	2.63	2.92	0.80	6.49	12.73
10.8	0.45	1.45	1.98	8.88	22.00	1.26	1.74	3.09	9.00	22.00

*Eddy parameters are given as a function of season (instead of month) in the Crutzen model. This parameterization is based on use of $\bar{\alpha}^{*2} = 0$ (Crutzen, 1980).

TABLE 2. SAMPLE EDDY PARAMETERS FOR WIDHOPF MODELS DURING SUMMER (AUGUST) IN NORTHERN HEMISPHERE AND WINTER IN SOUTHERN HEMISPHERE* (Source: Widhopf, 1978)

Altitude (km)	Summer (August), Latitude (deg.)					Winter (February), Latitude (deg.)				
	80^oN	60^oN	40^oN	20^oN	0	80^oN	60^oN	40^oN	20^oN	0
	Eddy Transport Coefficient K_{yy} (10^{10} cm^2/sec)									
20	0.29	0.28	0.19	0.12	0.17	3.76	2.97	0.83	0.27	0.17
18	0.34	0.38	0.39	0.21	0.21	3.37	2.90	1.17	0.70	0.21
16	0.42	0.52	0.63	0.30	0.25	2.99	2.87	1.61	1.18	0.25
14	0.63	1.03	1.27	0.42	0.34	2.77	3.22	2.91	2.13	0.34
12	0.85	1.54	1.90	0.55	0.43	2.54	3.57	4.21	3.09	0.43
10	1.61	2.20	1.71	0.40	0.32	3.21	4.94	5.62	2.67	0.32
	Slope of Mixing Axis, $\bar{\alpha}$ (10^{-4})									
20	-4.66	-14.57	- 9.63	-2.86	- 2.53	1.62	6.23	14.70	0.73	- 2.53
18	-5.97	-16.18	-15.95	-4.90	- 4.33	1.81	6.38	12.39	4.37	- 4.33
16	-6.60	-16.17	-15.87	-5.70	- 6.08	2.04	6.45	10.31	4.40	- 6.08
14	-6.92	-12.82	- 6.94	-5.36	- 9.65	2.89	7.52	5.53	3.10	- 9.65
12	-7.14	-11.95	- 3.99	-5.07	-11.74	3.90	8.40	3.68	-0.32	-11.74
10	0.62	0.16	0.58	2.50	- 1.89	-0.31	0.16	-0.18	-0.37	- 1.89
	Eddy Transport Coefficient K_{zz} (10^4 cm^2/sec)									
20	0.42	0.42	0.22	0.06	0.07	1.01	1.01	1.59	0.07	0.07
18	0.43	0.43	0.84	0.14	0.15	0.80	0.80	1.69	0.26	0.15
16	0.45	0.45	1.45	0.22	0.24	0.66	0.66	1.76	0.45	0.24
14	0.85	0.85	1.33	0.33	0.69	1.05	1.05	1.50	0.55	0.69
12	0.60	1.50	1.20	0.51	1.14	0.40	1.45	1.23	0.78	1.14
10	0.86	1.51	1.80	0.89	1.75	0.59	1.00	3.02	1.27	1.75

*The actual notation for the eddy coefficients in the Widhopf model is $K_{\phi\phi}$, $K_{z\phi}$ and K_{zz} (Widhopf, Glatt and Kramer, 1977). The angle $\bar{\alpha}$ is given here by the ratio $K_{z\phi}/K_{\phi\phi}$. The eddy coefficients in this model are given as a function of month for both northern and southern latitudes. Above data is applicable for the month of August; i.e., summer in the Northern Hemisphere and winter in the Southern Hemisphere. See text for the shift from southern (August) to northern (February) latitudes for winter.

TABLE 3. SAMPLE EDDY PARAMETERS DERIVED FROM POLEWARD TRANSPORT OF OZONE*
(Source: Danielsen and Louis, 1977)

Altitude (km)	Summer/Latitude (deg.) 80°N	60°N	40°N	20°N	0°	Winter/Latitude (deg.) 80°N	60°N	40°N	20°N	0°
	Eddy Transport Coefficient K_{yy}, (10^{10} cm^2/sec)									
25	0.13	0.17	0.10	0.12	0.15	0.40	0.44	0.20	0.15	0.15
20	0.19	0.43	0.11	0.17	0.25	0.33	0.54	0.24	0.15	0.25
15	0.16	0.25	0.11	0.28	0.61	0.24	0.40	0.33	0.21	0.61
10	0.20	0.21	0.13	0.38	1.04	0.32	0.49	0.34	0.23	1.04
	Slope of Mean Diffusion Axis, $\bar{\alpha}$ (10^{-4})									
25	5.15	6.29	2.84	-2.08	0.33	0.65	- 2.45	- 1.45	1.47	0.33
20	5.26	7.14	-12.18	-1.18	0.48	-3.00	-10.33	-20.92	-0.60	0.48
15	-0.38	9.60	11.73	-2.43	0.16	-7.96	-18.55	-29.61	-1.24	0.16
10	-1.25	2.48	1.08	-4.00	-0.16	0.44	- 4.55	- 6.21	4.22	-0.16
	Eddy Transport Coefficient, K_{zz}, (10^4 cm^2/sec)									
25	0.13	0.21	0.09	0.12	0.26	0.22	0.20	0.10	0.11	0.26
20	0.14	0.42	0.23	0.13	0.46	0.39	0.84	1.15	0.10	0.46
15	0.09	0.48	0.19	0.15	0.66	0.63	1.27	3.01	0.11	0.66
10	0.23	0.35	0.19	0.55	2.69	0.87	1.14	0.39	0.35	2.69

*Data is applicable to December-February; i.e., for summer in the Southern Hemisphere and winter in the Northern Hemisphere. See text for the switch in summer latitudes from south (December-February) to north (June-August).

It should be noted that the foregoing use of the time dependent continuity equation(s) for either chemical or inert tracers does not provide an independent additional constraint so as to fix a solution for the three unknown eddy coefficients from the two eddy tracer flux equations (4 and 5). As indicated by Eqs. (11) and (12), fundamental parameters in the Reed and German formulation are the statistics for the slope of mixing length paths or surfaces ($\bar{\alpha}$) and its eddy component or deviation from this average ($\bar{\alpha}^{*2}$). Therefore, the determination of the three eddy coefficients at given stratospheric meridional locations and month requires an additional constraint on these basic statistics by each parameterization. These constraints can be brought out by dividing Eq. (10) by the square of Eq. (8); after use of Eq. (7), the following result is obtained:

$$\frac{\bar{\alpha}^{*2}}{\bar{\alpha}^{2}} = \frac{K_{yy}K_{zz}}{K_{yz}^{2}} - 1 \qquad (13)$$

Equation (13) provides a common basis to compare the *implied* assumptions for the fundamental $\bar{\alpha}^{*2}$ statistics in the foregoing 2-D parameterizations of eddy transports. It is important to note that $\bar{\alpha}^{*2}/\bar{\alpha}^{2}$ is controlled only by the variability of the stratospheric winds (Eqs. 6), and that its magnitude must be always positive because it involves the ratio of two quadratic terms. Table 4 shows $\bar{\alpha}^{*2}/\bar{\alpha}^{2}$ values corresponding to the three parameterizations in Tables 1 to 3. The results in Table 4 indicate that these representative 2-D parameterizations fail to provide (a) positive values of $\bar{\alpha}^{*2}/\bar{\alpha}^{2}$ at every latitude and altitude and (b) nearly identical values for this ratio at a given location and season, as it should due to the dependence of $\bar{\alpha}^{*2}/\bar{\alpha}^{2}$ on the wind variability of the same stratosphere. Hence, these results indicate that the foregoing representative 2-D parameterizations of eddy transports are inconsistent both with the parent Reed and German formulation and among themselves.

TABLE 4. VALUES OF $\bar{\alpha}^{*2}/\bar{\alpha}^2$ FOR THREE 2-D PARAMETERIZATIONS OF EDDY TRANSPORTS.

CRUTZEN* (Table 1)

ALTITUDE (km)	SUMMER, LATITUDE (deg)					WINTER, LATITUDE (deg)				
	80°N	60°N	40°N	20°N	0°	80°N	60°N	40°N	20°N	0°
19.8	1.2	0.3	0.1	2.4	443.4	0.1	0.2	-0.1	1.7	530.0
18.0	0.8	0.2	0.1	36.7	532.3	0.7	0.1	-0.2	171.9	562.1
16.3	0.6	0.1	0.3	4894.8	96644.1	0.5	0	-0.6	1986.6	110630.0
14.5	0.4	0.1	3.4	27515.2	101642.6	0.4	-0.1	811.7	818.4	470051.1
12.7	0.4	5.6	58.8	1488.5	115924.9	0.3	-0.2	1.1	235827.5	1657551.1
10.8	7.0	64.8	129.2	461.7	565842.6	0.1	302.4	7.1	1065.4	2864582.3

WIDHOPF (Table 2)

ALTITUDE (km)	SUMMER, LATITUDE (deg)					WINTER, LATITUDE (deg)				
	80°N	60°N	40°N	20°N	0°	80°N	60°N	40°N	20°N	0°
20	5.7	-0.3	0.3	5.1	5.4	9.2	-0.1	-0.1	47.7	5.4
18	2.6	-0.6	-0.1	1.8	2.8	6.3	-0.3	-0.1	0.9	2.8
16	1.5	-0.7	-0.1	1.3	1.6	4.3	-0.4	0	1.0	1.6
14	1.8	-0.5	1.2	1.7	1.2	3.5	-0.4	0.7	1.7	1.2
12	0.4	-0.3	3.0	2.6	0.9	0	-0.4	1.2	245.5	0.9
10	138.0	2680.1	311.9	34.6	152.1	190.3	789.7	1657.5	346.4	152.1

DANIELSEN/LOUIS (Table 3)

ALTITUDE	SUMMER, LATITUDE (deg)					WINTER, LATITUDE (deg)				
	80°N	60°N	40°N	20°N	0°	80°N	60°N	40°N	20°N	0°
25	2.8	2.1	10.2	22.1	1590.7	129.2	6.6	22.8	32.9	1590.7
20	1.7	0.9	0.4	53.9	797.6	12.1	0.5	0.1	184.2	797.6
15	388.5	1.1	0.3	8.1	4225.4	3.1	-0.1	0	33.1	4225.4
10	72.6	26.1	124.3	8.1	10102.7	1403.3	10.2	2.0	7.6	10102.7

*Since the Crutzen model used $\bar{\alpha}^{*2} = 0$ (Crutzen, 1980), then Eq. (13) yields $K_{yy}K_{zz}/K_{yz}^2 = 1$. The data in Table 1 shows that neither of these two conditions holds at low latitudes (Hidalgo, 1978). The above differences between the Crutzen and Widhopf values at low latitudes may help explain the difference in interhemispheric aircraft effects on ozone from these models.

A consequence of the former result is that such parameterizations may not then use the Reed and German (1965) formulation to imply physical justification of their prognostic utility for viable forecasting of anthropogenic ozone effects.

IV. APPARENT UNDETERMINABILITY OF BASIC $\bar{\alpha}^{*2}$ STATISTICS

The foregoing 2-D parameterizations of eddy transports had to contend with the solution of an undetermined system of two equations (4 and 5) and three unknowns (K_{yy}, K_{yz}, K_{zz}). The solution of such a system required then additional constraints involving implied assumptions for $\bar{\alpha}^{*2}/\bar{\alpha}^2$ as given by Eq. (13). However, a straightforward alternative procedure would consist in a direct determination of the $\bar{\alpha}$ and $\bar{\alpha}^{*2}$ statistics, which would be derivable from the Reed and German Eqs. (6), i.e.

$$\tan \alpha = \frac{w^*}{v^*} = \frac{w - \bar{w}}{v - \bar{v}} \quad , \qquad (14)$$

where α (θ, λ, z, t) is the slope of mixing length paths or surfaces as a function of latitude (θ), longitude (λ), altitude (z), and time (t, in hours). Equation (14) indicates the following: (1) α is a function of the variability of the vertical and meridional winds in the stratosphere, (2) α would be determined from corresponding wind data (w, v) in the stratosphere, and (3) α^* would be derivable from α in the same manner as the eddy winds. Because of the unmeasurability of the very small vertical winds, they must always be *calculated*, taking into account radiation effects in the stratosphere. It must thus be emphasized that any indirect method to determine the vertical transports from *observations* of the horizontal winds and temperature fields would require the use of assumptions, including those for radiation effects in the stratosphere. Since 3-D GCM wind data already include diabatic effects in the solution of the primitive equations, it would be possible to use such wind data together with Eq. (14) so as to derive estimators

of the $\bar{\alpha}$ and $\bar{\alpha}^{*2}$ statistics as a function of latitude, altitude, and month. Wind data from the Geophysical Fluid Dynamics Laboratory (GFDL)/GCM at six-hour intervals for each month was available for this purpose. The basic characteristics of this GCM have been described by Holloway and Manabe (1971), Manabe and Holloway (1975), and Manabe and Mahlman (1976). This GCM is characterized by (a) consideration of seasonal effects; (b) a high horizontal resolution of about 265 km, which is important for tracer transports by wave numbers $\eta > 10$ (Mahlman, 1975); and (c) a vertical resolution of about 3 km from the lower stratosphere to the middle troposphere.

However, basic difficulties in the application of Eq. (14) were found to be: (1) the fact that whenever v^* decreases faster than w^*, the absolute magnitude $|\alpha|$ of the angle of the mixing length path becomes relatively large and (2) the statistics of $\bar{\alpha}$ and $\bar{\alpha}^{*2}$ would become then dominated by few large values of $|\alpha|$. These results are illustrated in Tables 5 through 7 for low (24° N), middle (48° N), and high (72° N) latitudes, respectively. The data in each of these tables are based on *sample* GFDL/GCM wind data for a 6-hour period (See Appendix). These tables show the dominance of a few large angles on the zonal averages of $[\alpha]$ and $[\alpha^{*2}]$ as a function of pressure level in the critical region for the exchange of tracers between the lower stratosphere and upper troposphere. Each table shows (1) the largest absolute magnitude of α (or $|\alpha_{max}|$) that takes place along discrete longitudinal points for a given latitude and pressure level; (2) the number of longitudinal points at each latitude and pressure level, depending on the magnitude of $|\alpha|$, i.e., (a) for all magnitudes including those for $|\alpha_{max}|$, and (b) excluding angles that are larger than either, say, 5 or 1 deg; and (3) the corresponding $[\alpha]$ and $[\alpha^{*2}]/[\alpha]^2$ values when including $|\alpha_{max}|$ or excluding ($|\alpha| \leq 5$, 1 deg) large magnitudes of $|\alpha|$. Thus, Table 5 shows that at 24° N latitude in the *tropopause*

TABLE 5. SAMPLE [α], [α^{*2}] AT 24°N LATITUDE

$|\alpha_{max}|$ AND NUMBER OF LONGITUDINAL POINTS AS FUNCTION OF $|\alpha|$

	PRESSURE LEVEL, mbar(km)			
	38(22.4)	65(19)	110(15.6)	190(12.1)
$\|\alpha_{max}\|$, deg	3.1	14.9	71.4	10.3
$\|\alpha\| \leq \|\alpha_{max}\|$, pts	138	138	138	138
$\|\alpha\| \leq 5$ deg, pts	138	133	135	137
$\|\alpha\| \leq 1$ deg, pts	131	126	131	123
ZONAL AVERAGE [α](10^{-4})				
$\|\alpha\| \leq \|\alpha_{max}\|$	-3.7	5.0	99.8	1.2
$\|\alpha\| \leq 5$ deg	-3.7	4.5	7.2	-11.9
$\|\alpha\| \leq 1$ deg	3.0	-0.5	7.9	-9.2
[α^{*2}]/[α]^2				
$\|\alpha\| \leq \|\alpha_{max}\|$	544.4	5254.0	149.7	26861.1
$\|\alpha\| \leq 5$ deg	544.4	282.5	148.5	126.5
$\|\alpha\| \leq 1$ deg	250.4	11642.5	35.5	31.4

TABLE 6. SAMPLE [α], [α^{*2}] AT 48°N LATITUDE

$|\alpha_{max}|$ AND NUMBER OF LONGITUDINAL POINTS AS FUNCTION OF $|\alpha|$

	PRESSURE LEVEL, mbar(km)			
	38(22.4)	65(19)	110(15.6)	190(12.1)
$|\alpha_{max}|$, deg	6.9	14.9	6.2	4.8
$|\alpha| \leq |\alpha_{max}|$, pts	99	99	99	99
$|\alpha| \leq$ 5 deg, pts	98	96	98	99
$|\alpha| \leq$ 1 deg, pts	89	94	96	93

ZONAL AVERAGE [α](10^{-4})

$|\alpha| \leq |\alpha_{max}|$	-31.1	55.7	-7.8	-2.7
$|\alpha| \leq$ 5 deg	-19.2	-7.7	2.8	-2.7
$|\alpha| \leq$ 1 deg	-0.7	-8.8	2.9	-4.7

[α^{*2}]/[α]^2

$|\alpha| \leq |\alpha_{max}|$	26.2	46.6	232.8	1687.8
$|\alpha| \leq$ 5 deg	31.4	63.0	314.7	1687.8
$|\alpha| \leq$ 1 deg	2477.3	26.6	185.4	34.8

TABLE 7. SAMPLE $[\alpha]$, $[\alpha^{*2}]$ AT 72°N LATITUDE

$|\alpha_{max}|$ AND NUMBER OF LONGITUDINAL POINTS AS FUNCTION OF $|\alpha|$

	PRESSURE LEVEL, mbar(km)			
	38(22.4)	65(19)	110(15.6)	190(12.1)
$\lvert\alpha_{max}\rvert$, deg	1.2	18.1	0.7	1.4
$\lvert\alpha\rvert \le \lvert\alpha_{max}\rvert$, pts	45	45	45	45
$\lvert\alpha\rvert \le 5$ deg, pts	45	44	45	45
$\lvert\alpha\rvert \le 1$ deg, pts	43	43	45	44

ZONAL AVERAGE $[\alpha](10^{-4})$

$\lvert\alpha\rvert \le \lvert\alpha_{max}\rvert$	-13.0	-75.8	-3.4	2.2
$\lvert\alpha\rvert \le 5$ deg	-13.0	-7.8	-3.4	2.2
$\lvert\alpha\rvert \le 1$ deg	-13.9	-12.6	-3.4	-3.4

$[\alpha^{*2}]/[\alpha]^2$

$\lvert\alpha\rvert \le \lvert\alpha_{max}\rvert$	19.0	37.9	52.4	360.1
$\lvert\alpha\rvert \le 5$ deg	19.0	23.7	52.4	360.1
$\lvert\alpha\rvert \le 1$ deg	8.0	2.7	52.4	32.8

region (110 mbar or 15.6 km), the largest absolute magnitude of α is as high as 71.4 deg for 138 discrete longitudinal points at this latitude; however, the bulk of the data (135 points or 98 percent) had α values smaller than 5 deg. The corresponding results for $[\alpha]$ show that its magnitude drops from 99.8×10^{-4} to 7.2×10^{-4} when excluding only 2 percent of the data with angles $|\alpha|$ larger than 5 deg.* Similar results are obtained above or below the tropopause. At 65 mbar (19 km), the $[\alpha^{*2}]/[\alpha]^2$ values drop from 5254.0 to 282.5 when excluding 4 percent of the data with $|\alpha| > 5$ deg; whereas at 190 mbar (12.1 km), $[\alpha^{*2}]/[\alpha]^2$ drops from 26861.1 to 126.5 when excluding only 1 percent of the data with $|\alpha| > 5$ deg.

The data in Tables 6 and 7 show that the number of discrete longitudinal points in the numerical grid of the GCM for a given latitude decreases as the latitude increases. Table 6 indicates that (1) $|\alpha_{max}|$ at 48° N and 65 mbar (19 km) is 14.9 deg and (2) the magnitude of $[\alpha]$ drops from 55.7×10^{-4} to -7.7×10^{-4} when excluding only 3 percent of the data with $\alpha \geq 5$ deg. Table 7 shows similar corresponding results at 72° N and the same pressure level of 65 mbar (19 km). Thus, the results in Tables 5 through 7 indicate that the estimators for the $\bar{\alpha}$ and $\bar{\alpha}^{*2}$ statistics would be dominated by a small percent of data characterized by large absolute magnitudes of α. Hence, the use of the full ensemble of 120 sets of 6-hr-period GCM wind data for each stratospheric meridional location and month could not be justified.

The foregoing results in Tables 5 through 7 are obtained from a *strict* use of the Reed and German Eqs. (6) for the α statistics and use of sample GCM wind data for a 6-hour period, which might be somewhat noisy due to the rather low vertical resolution.

*Note, from Eq. (14), that $|\alpha|$ depends on $\bar{w}$ and $\bar{v}$; which in turn depends on the number of discrete points dropped from the data. A computer code to process the data is also given in the Appendix.

of the GCM model. Therefore, a determination of the three fundamental parameters (K_{yy}, $\bar{\alpha}$, $\bar{\alpha}^{*2}$) in the basic Reed and German formulation (Eqs. 7 through 10) would require both reinterpretation of basic relevant concepts for the calculation of such statistics and reformulation of the current methodology that uses the flux equations (Eqs. 4 and 5) for determining the magnitude of the eddy transports coefficients illustrated in Tables 1 to 3.

V. REED AND GERMAN CONSTRAINTS CARRIED OVER TO TWO-DIMENSIONAL PHOTOCHEMICAL MODELS

A need for reformulation of the current methodology for establishing both the magnitude and even nature of 2-D eddy transport coefficients is emphasized by the following:

(1) Even if the $\bar{\alpha}$ and $\bar{\alpha}^{*2}$ statistics were determinable from wind data through Eq. (6), the system of Eqs. (7) through (10) would then specify K_{yz} and K_{zz} in terms of K_{yy}; which could be determined from Eq. (4). The result would be an overspecified system of two equations (4 and 5) for one unknown (K_{yy}) instead of the undetermined system of two equations (4 and 5) and three unknowns (K_{yy}, K_{yz}, K_{zz}), as dealt with in the current methodology for the 2-D parameterizations of tracer transports in Tables 1 through 3.

(2) As shown by Andrews and McIntyre (1976), Eq. (3) is valid for waves with small amplitudes. However, as pointed out by Holton (1980), ℓ_y and ℓ_z are to be interpreted as fluid particle displacements caused by the waves. Hence, if v* and w* denote the wave velocity components

$$v^* = \frac{d\ell_y}{dt} \quad , \qquad w^* = \frac{d\ell_z}{dt} \quad . \tag{15}$$

Then, in place of Eqs. (7) through (10) the following result is obtained

$$K_{yy} = \overline{v^* \ell_y} = \overline{\ell_y \frac{d\ell_y}{dt}} = \frac{1}{2} \frac{\overline{d\ell_y^2}}{dt} \tag{16}$$

$$K_{yz} = \overline{v^* \ell_z} = \overline{\ell_z \frac{d\ell_y}{dt}} \tag{17}$$

$$K_{zy} = \overline{w^* \ell_y} = \overline{\ell_y \frac{d\ell_z}{dt}} = \frac{d}{dt} (\overline{\ell_y \ell_z}) - K_{yz} \tag{18}$$

$$K_{zz} = \overline{w^* \ell_z} = \overline{\ell_z \frac{d\ell_z}{dt}} = \frac{1}{2} \frac{\overline{d\ell_z^2}}{dt} \tag{19}$$

Equation (18) shows that, in general, $K_{zy} \neq K_{yz}$; a result that is different from the Reed and German Eq. (9), which is derived from the critical assumption that α^* is independent of v and ℓ.

The foregoing results indicate that the reformulation of the methodology to derive 2-D eddy coefficients may further involve the determination of the four parameters given by Eqs. (16) through (19), instead of the three in the Reed and German Eqs. (7) through (10). *These results indicate again that the current 2-D diagnostic parameterizations of stratospheric tracer transports (as illustrated in Tables 1 through 3), based on Eqs. (7) through (10) or Eq. (9) with (4), (5), and (2) for either inert or chemically active tracers, may not rely on the parent Reed and German (1965) formulation to justify their prognostic use in the forecasting of adverse anthropogenic effects on atmospheric ozone.*

VI. PAST INTERPRETATIONS OF REED-GERMAN RESULTS

Previous attempts (Mahlman, 1975; Hidalgo, 1978) to assess the *prognostic* validity of diffusivity concepts used in 2-D parameterizations of tracer transports in the stratosphere have been based on GFDL GCM/tracer model data for a tracer characterized as being chemically inert in the stratosphere but with heterogeneous sinks in the troposphere. The GCM/tracer model combines the GCM numerical solutions from the primitive equations with those from the 3-D continuity Eq. (1) for a chemically inert tracer, i.e., the auxiliary tracer model solves for the time evolutions of tracers from $dR/dt = 0$ while using as inputs the wind field of the parent GCM. Because of constraints on computer resources, the same annual cycle from the GCM is reused in subsequent cycles of the tracer model. While this procedure does not allow use of the annual variability of the wind fields, the annual variability of the tracer is soley due to the tracer itself. The GCM/tracer model data used to assess the prognostic validity of diffusivity concepts in 2-D parameterizations have then come from the following three numerical experiments:

(1) A "vertical stratification" experiment, which utilized a tracer-source in the upper stratosphere. This was the earliest ozone-precursor numerical experiment that was designed to provide a crude simulation of the equilibrium photochemical stratification of ozone. It specified a constant mixing ratio in the upper stratosphere of a chemically inert tracer, which was assumed to have heterogeneous sinks in the lower troposphere for its removal by rainout processes (Mahlman, 1973a, 1975).

(2) A "mid-latitude point source" experiment, which utilized an instantaneous release of a chemically inert tracer at a point located at a middle northern latitude in the lower stratosphere. This experiment simulated the distributions of radioactive nuclear debris in the stratosphere from a nuclear explosion. It specified an initial distribution of mixing ratio at and near the point-source of a tracer, which was again characterized as being chemically inert in the stratosphere but with heterogeneous sinks in the troposphere. (Mahlman, 1973a, 1975; Mahlman and Moxim, 1978).

(3) An SST (supersonic transport)-like experiment, which utilized constant-line sources of a chemically inert tracer located at specified zonal segments at a northern middle latitude in the lower stratosphere (Mahlman, 1973b, 1978; Hidalgo, 1978). This experiment simulated the time (years) evolutions of the monthly distribution of, say, NO_y ($NO + NO_2 + 2N_2O_5 + NO_3 + HNO_3$) as the result of emissions of SST engine effluents in the lower stratosphere. Again, the characteristics of the inert tracers are as in the foregoing two experiments.

The approach used in these assessments of the prognostic validity of 2-D parameterizations of eddy transports consisted in the use of the Reed and German Eqs. (4), (5), and (9), together with 3-D GCM/tracer model data from the above numerical experiments. The 3-D tracer data was averaged using the $(\bar{\ })$ operator to obtain estimators for the 2-D tracer statistics of the meridional and vertical eddy transports and corresponding gradients of mixing ratio. However, this use of the Reed and German equations with averaged 3-D GCM/tracer model data could not overcome the difficulty of defining properly the magnitude of the $\bar{\alpha}$ and $\bar{\alpha}^{*2}$ statistics; i.e., the problems faced previously

when attempting to solve the undetermined system of the two eddy flux equations for the three unknown eddy coefficients.

Since Eq. (14) yields $\alpha = w^*/v^*$ for small angles of α, an approximation used to estimate $\bar{\alpha}$ was to multiply the numerator and denominator of α by R^* and assume that $\bar{\alpha} = \overline{w^*R^*}/\overline{v^*R^*}$. Use of Eqs. (4), (5), and (9) yielded then (Mahlman, 1975):

$$K_{yy} = - \frac{\overline{v^*R^*}^2}{\overline{v^*R^*}\,\frac{\partial\bar{R}}{\partial y} + \overline{w^*R^*}\,\frac{\partial\bar{R}}{\partial z}} , \qquad (20)$$

and

$$K_{zz} = - \frac{\overline{w^*R^*}^2}{\overline{v^*R^*}\,\frac{\partial\bar{R}}{\partial y} + \overline{w^*R^*}\,\frac{\partial\bar{R}}{\partial z}} . \qquad (21)$$

The use of Eqs. (20), (21) and averaged 3-D GCM/tracer data for the eddy transports and gradients of mixing ratio in these equations would then yield the magnitude of the eddy transport coefficients. Such results, based on the "vertical stratification" and "mid-latitude point source" experiments, indicated that there were regions in the stratosphere where the eddy transport coefficients became even *negative* (Mahlman, 1975); results that were also confirmed for both the mid-latitude or instantaneous-point source as well as the constant-line or SST sources as indicated in Tables 8 through 10 (Hidalgo, 1978). However, these latter results also indicated that the corresponding magnitudes of $\bar{\alpha}$ became different for the point source and constant-line source experiments (Table 8) at the same stratospheric location and month (season) instead of remaining fixed by the variability of the stratospheric winds as by Eq. (14). Furthermore, since division of Eq. (21) by (20) yields

TABLE 8. SLOPE OF MIXING LENGTH PATH AS GIVEN BY PRIMITIVE EQUATIONS, α (10-4)*

Source: Mahlman, Private Communication, 1978

Level, mbar	Standard Height, km	Latitude 72°N	48°N	24°N	0	24°S	48°S	72°S
		Instantaneous Injection, Winter (December), Fourth Year						
38	22.4	- 3.8	- 31.6	10.3	8.9	- 42.0	20.5	-132.0
65	19.0	- 6.4	- 31.2	7.2	- 1.4	- 39.4	23.5	-256.0
110	15.6	- 41.1	- 42.0	23.3	254.0	- 21.6	32.5	+231.0
190	12.1	- 20.1	- 26.5	84.2	18.0	+116.0	67.6	-525.0
315	8.9	-235.0	- 41.1	287.0	44.1	-281.0	-202.0	+844.0
		SST Injections, Winter (December), Fifth Year						
38	22.4	8.1	46.8	- 3.5	0.2	-102.0	- 5.9	- 56.1
65	19.0	46.4	13.2	- 1.7	1.9	-136.0	1.2	- 89.1
110	15.6	13.2	- 19.5	- 1.0	18.9	- 30.0	8.3	+188.0
190	12.1	- 10.2	- 25.3	19.4	76.1	27.7	70.7	-547.0
315	8.9	53.9	- 20.9	79.5	73.9	99.5	53.5	+640.0
		SST Injections, Summer (June), Fifth Year						
38	22.4	- 8.0	- 6.0	- 95.7	- 9.8	- 20.3	8.1	- 93.4
65	19.0	+ 13.2	+ 0.4	+ 3.5	3.2	+ 40.6	10.6	- 60.4
110	15.6	- 7.0	-2630.0	+ 15.1	23.1	- 98.4	8.7	30.7
190	12.1	- 89.6	- 7.9	- 43.2	84.6	32.3	1880.0	91.0
315	8.9	+ 3.4	48.1	+166.0	314.0	51.3	5.2	114.0

*For instantaneous injection at 38 mbar and 72°N, for example, [α] = -3.8×10^{-4}.

TABLE 9. VERTICAL EDDY COEFFICIENTS AS GIVEN BY PRIMITIVE EQUATIONS, K_{zz} ($10^4 cm^2/sec$)*

(Source: Mahlman, Private Communication, 1978)

Level, mbar	Standard Height, km	Latitude 72°N	48°N	24°N	0	24°S	48°S	72°N
		Instantaneous Injections, Winter (December), Fourth Year						
38	22.4	6.4(-1)	-1.6(1)	1.5(0)	9.6(-2)	4.0(-1)	1.2(0)	-3.0(0)
65	19.0	1.9(-1)	-5.7(1)	4.6(-1)	8.8(-3)	9.2(-2)	4.7(-1)	-2.5(0)
110	15.6	7.5(-1)	+3.4(2)	1.3(0)	-4.9(-2)	9.0(-1)	6.6(-1)	-6.0(0)
190	12.1	8.0(-1)	+6.3(0)	4.4(0)	-1.2(-1)	2.1(0)	8.0(-1)	-7.8(0)
315	8.9	1.3(0)	+3.7(0)	2.6(1)	-1.9(0)	6.0(0)	2.9(0)	-2.4(1)
		SST Injections, Winter (December), Fifth Year						
38	22.4	3.4(-1)	-1.6(0)	1.8(-1)	1.0(-4)	1.1(0)	1.3(-1)	-2.0(0)
65	19.0	9.3(-1)	-3.3(1)	6.8(-2)	1.7(-2)	1.5(-1)	9.3(-3)	-1.7(0)
110	15.6	1.3(-1)	-1.3(1)	8.2(-3)	2.7(0)	9.0(-1)	1.5(-1)	-4.4(0)
190	12.1	3.6(-1)	+1.5(0)	4.7(-1)	3.4(0)	1.4(0)	3.9(-1)	-6.7(0)
315	8.9	1.5(0)	+6.6(0)	5.7(0)	7.3(0)	3.4(0)	2.2(0)	-2.2(1)
		SST Injections, Summer (June), Fifth Year						
38	22.4	1.4(-1)	2.4(-1)	3.1(0)	1.1(-1)	8.0(-1)	-1.0(0)	-1.2(0)
65	19.0	3.9(1)	2.9(-3)	1.8(-1)	3.1(-2)	4.9(-1)	5.5(-1)	-2.1(-1)
110	15.6	-1.9(0)	8.8(-1)	9.6(-1)	2.6(0)	1.1(0)	1.5(0)	-3.1(-1)
190	12.1	+3.3(-1)	6.4(-1)	2.1(0)	4.7(0)	1.4(0)	4.5(-1)	-2.4(0)
315	8.9	-1.5(-3)	1.2(0)	9.9(0)	3.2(1)	2.0(0)	-7.1(-1)	-1.1(1)

*For instantaneous injection at 38 mbar and 72°N, for example, $K_{zz} = 6.4(10^{-1}) \cdot 10^4 = 6.4 \times 10^3$ cm^2/sec. Note that (0) denotes 10^0.

TABLE 10. HORIZONTAL EDDY COEFFICIENT, AS GIVEN BY PRIMITIVE K_{yy} (10^{10} cm^2/sec)*

(Source: Mahlman, Private Communication, 1978)

Level, mbar	Standard Height, km	Latitude 72^oN	48^oN	24^oN	0	24^oS	48^oS	72^oS
		Instantaneous Injections, Winter (December), Fourth Year						
38	22.4	4.5(0)	-1.6(0)	1.4(0)	1.2(-1)	2.3(-2)	2.8(-1)	-1.7(-2)
65	19.0	4.6(-1)	-5.8(0)	9.0(-1)	4.4(-1)	5.9(-3)	8.6(-2)	-3.8(-3)
110	15.6	4.4(-2)	+1.9(1)	2.4(-1)	-7.6(-5)	1.9(-1)	6.2(-2)	-1.1(-2)
190	12.1	2.0(-1)	+8.9(-1)	6.2(-2)	-3.7(-2)	1.6(-2)	1.7(-2)	-2.8(-3)
315	8.9	2.3(-3)	+2.2(-1)	3.1(-2)	-9.8(-2)	7.6(-3)	7.2(-3)	-3.4(-3)
		SST Injections, Winter (December), Fifth Year						
38	22.4	5.2(-1)	-7.2(-2)	1.5(0)	2.2(-1)	1.0(-2)	3.7(-1)	-6.5(-2)
65	19.0	4.3(-2)	-1.9(1)	2.5(0)	4.5(-1)	8.1(-4)	6.3(-1)	-2.1(-2)
110	15.6	7.3(-2)	-3.5(0)	8.4(-1)	7.5(-1)	1.0(-1)	2.2(-1)	-1.2(-2)
190	12.1	3.5(-1)	+2.3(-1)	1.3(-1)	5.9(-2)	1.9(-1)	7.8(-3)	-2.3(-3)
315	8.9	5.3(-2)	+1.5(0)	9.0(-2)	1.3(-1)	3.5(-2)	7.6(-2)	-5.5(-3)
		SST Injections, Summer (June), Fifth Year						
38	22.4	2.2(-1)	6.7(-1)	3.4(-2)	1.2(-1)	1.9(-1)	-1.6(0)	-1.4(-2)
65	19.0	2.2(1)	1.5(0)	1.5(0)	3.1(-1)	3.0(-2)	4.9(-1)	-5.8(-3)
110	15.6	-3.8(0)	1.3(-5)	4.2(-1)	4.9(-1)	1.1(-2)	1.9(0)	-3.2(-2)
190	12.1	+4.1(-3)	1.0(0)	1.2(-1)	6.6(-2)	1.4(-1)	1.3(-5)	-2.9(-2)
315	8.9	-1.2(-2)	5.0(-2)	3.6(-2)	3.3(-2)	7.5(-2)	-2.6(0)	-8.8(-2)

*For instantaneous injection at 38 mbar and 72^oN, for example, $K_{yy} = 4.5(10^0) \cdot 10^{10} = 4.5 \times 10^{10}$ cm^2/sec. Note that (0) denotes 10^0.

$K_{zz}/K_{yy} = \bar{\alpha}^2$, the use of Eqs. (7) and (8) gives then $K_{yy}K_{zz}/K_{yz}^2 = 1$. Hence, Eq. (13) indicates that the assumption $\bar{\alpha} = \overline{w^*R^*}/\overline{v^*R^*}$ leads to $\bar{\alpha}^{*2} = 0$. Since the use of Eqs. (20) and (21) contradicts both the sole dependency of $\bar{\alpha}$ on the wind variability as well as the apparent undeterminability of $\bar{\alpha}^{*2}$ from wind data, previous conclusions of negative eddy transport coefficients based on these equations are not warranted from a strict use of the Reed and German formulation.

It should however be noted that the foregoing implied assumption of $\bar{\alpha}^{*2} = 0$ in Eqs. (20) and (21), as well as the results of Tables 8 through 10 is as in the Crutzen model at middle and high latitudes (Table 1). On this basis, it appears that the use of $\bar{\alpha}^{*2} = 0$ in diagnostic parameterizations (for a stratosphere without SST pollutants) would likewise yield $\bar{\alpha}$ values that are inconsistent with those required by the Reed and German equations for a stratosphere with SST pollutants (Table 8); i.e., such diagnostic parameterizations with fixed $\bar{\alpha}$ values at a given stratospheric location and month (season) may have a questionable prognostic value. Furthermore, the validity of even the diagnostic value of 2-D parameterizations based on $\bar{\alpha}^{*2} = 0$ are open to question, since the foregoing use of GCM/tracer model data together with the Reed and German equations requires that the eddy coefficients may become negative (Tables 9, 10). Moreover, it is of interest to indicate that GCM/tracer model data suggest that the magnitude of the tracer eddy transports may depend on the prevailing time and/or space tracer configuration in the stratosphere (Mahlman and Moxim, 1978; Hidalgo, 1978); a result that would affect the accuracy of diagnostic 2-D parameterizations (Tables 2, 3) that are not based on $\bar{\alpha}^{*2} = 0$.

VII. OUTLOOK FOR PROGRESS IN PROGNOSTIC 2-D FORMULATIONS OF TRACER TRANSPORTS

Recent developments stemming from a Lagrangian instead of a Eulerian description of wave motions and associated mean flows (Andrews and McIntyre, 1978 a and b; Dunkerton, 1978) indicate that (a) the net countergradient "diffusion" is really an advection by the Stoke's drift due to the waves (Wallace, 1978); (b) the entire bulk motion of the center of mass of air parcels and tracers would be described advectively, not by K_{yz} slantwise diffusion; however there is still need for diffusion to explain the lateral and vertical spread of a tracer about its center of mass (Holton, 1980); and (c) the Reed and German form of Eqs. (4) and (5) might be retainable for small-amplitude waves. However, a rather drastic reinterpretation of the physical meaning of Eqs. (4) and (5) becomes necessary (Plumb, 1979; Matsuno, 1980); namely, major parts of the meridional eddy fluxes of ozone, potential temperature, and other vertically stratified quantities would be the result of a systematic correlation between the vertical displacement and the meridional velocity of air parcels arising from a particular structure of planetary waves, and hence the fluxes are nearly transverse-gradient rather than obliquely down-gradient (Clark and Rogers, 1978). Such eddy transports are shown to be nearly advective instead of diffusive in nature and may be expressed by eddy transport coefficients with $K_{yz} \neq K_{zy}$.

The foregoing possibility is suggested from exploratory investigations that considered the stratospheric motions induced by an upward, steady-state propagation of a planetary wave from the troposphere into a stratosphere characterized by

a uniform zonal (i.e. $\bar{u}$ or eastward) circulation in a latitude domain (Matsuno, 1980). The approach consisted in obtaining (1) solutions of the potential vorticity equation for the wave structure and the induced motions in the stratosphere, (2) Lagrangian trajectories of the air parcel motions and (3) eddy transports of χ (e.g. ozone) carried by the air parcels in a form which is proportional to local gradients of χ as in Eqs. (4) and (5). The important relevant results from this mechanistic approach are then as follows: (1) the Lagrangian trajectories of air parcels consists of cyclic motions along ellipses as well as the linear motions (as shown in Fig. 1) in the meridional domain of the stratosphere, (2) the orientation of the major axis of the meridional ellipses is indeed as that of $\bar{\alpha}$ in Fig. 1 and with the same order of magnitude ($\sim 10^{-4}$) as in the Reed and German concept, (3) if the meridional ellipses were superimposed on Fig. 1, the direction of motion of air parcels would be clockwise at any latitude, (4) the eddy transport coefficients may be expressed in terms of gradients as in Eqs. (4) and (5) but with unequal K_{yz} and K_{zy} coefficients and (5) the eddy transport coefficients are a function of the period of the cyclic motions along the ellipses and the time constant of chemical adjustment. Hence, these encouraging exploratory results suggest that a *prognostic* 2-D formulation of eddy transports of chemically inert or active tracers in the stratosphere might be feasible.

VIII. TESTS OF 1-D PARAMETERIZATIONS

The 1-D photochemical models of the stratosphere and troposphere have played a dominant role during recent years in crude assessments of ozone effects from emissions of (1) aircraft engine effluents at high altitudes [Grobecker et al., 1974; National Academy of Sciences (NAS), 1975; Oliver et al., 1977; Broderick, 1977] and (2) chlorofluoromethanes (CFMs) at the earth's surface (NAS, 1976; NASA, 1977; Crutzen et al., 1977). Basic factors for the popularity of 1-D photochemical models have been the uncertain knowledge of the relevant chemistry together with their capability for a wide coverage of chemical cycles and species as a result of their rather modest requirements for computer and manpower resources.

The 1-D continuity equations for the conservation of chemical species are obtained by taking the global-annual statistical average of Eqs. (1) for an ensemble of many years. If $\{(\ )\}$ denotes the global-annual ensemble average of ( ), then $\{(\ )\}$ represents a generalization of the 2-D ensemble average $(\bar{\ })$ by extending it with respect to latitude and even time from a monthly to an annual basis. Although it would be possible to likewise define $(\ )^{**} = (\ ) - \{(\ )\}$ so as to separate at each altitude the 1-D average of the vertical eddy transports of mixing ratio $\{w^{**}R^{**}\}$ from those of the corresponding vertical winds or 1-D circulation $\{w\}\{R\}$, it is customary to extend the concept of 2-D eddy transports to the 1-D case by assuming that the 1-D transport coefficient K_z (or K_p) includes now the transports by the 1-D vertical circulation. Since $\{\vec{\nabla}_p \cdot R_1\vec{U}\} = 0$, where $\vec{U}$ denotes the local horizontal wind vector, the basic continuity equations for 1-D photochemical models in pressure coordinates is given by

$$\frac{\partial}{\partial t}\{R_1\} + \frac{\partial}{\partial p}\{\omega R_1\} = \{P_1\} - \{L_1\} \quad , \qquad (22)$$

where p denotes pressure and $\omega = dp/dt$. Again, with

$$\{\omega R_1\} = - K_p \frac{\partial}{\partial p}\{R_1\} \ , \qquad (23)$$

where K_p is given in $(\text{mbar})^2/\text{sec}$, Eq. (22) becomes a set of differential equations for the mixing ratio R_1. The above equations can be written in the traditional altitude instead of pressure coordinate through use of the hydrostatic equation. The 1-D result equivalent to that of Eq. (2) for a chemically inert tracer in the stratosphere takes then the following form:

$$\frac{\partial}{\partial t}\{R\} = - \frac{1}{\tilde{\rho}} \frac{\partial}{\partial z} \tilde{\rho} \{wR\} \quad , \qquad (24)$$

where $\tilde{\rho}$ is proportional to $\{p/T\}$. Equation (23) becomes

$$\{wR\} = - K_z \frac{\partial}{\partial z}\{R\} \quad . \qquad (25)$$

Since 1-D photochemical models assume that the 1-D transport of chemical species is given by Eq. (25) for a chemically inert tracer, it is seen that the usual definition of the 1-D transport coefficient $K_z(z)$ is given as a ratio of the global-annual ensemble average of the flux of mixing ratio by both the vertical components of the circulation and eddy motions to the vertical gradient of the corresponding average of mixing ratio. The lack of worldwide observations for an ensemble of many annual cycles of a suitable tracer in the critical regions of the lower stratosphere and upper troposphere has made it very difficult to arrive at a generally acceptable $K_z(z)$ profile for the forecasting of long-range adverse anthropogenic 1-D ozone effects.

The continuity equations of 1-D photochemical models have the form of Eqs. (24) and (25), except that R_1 replaces R and the right-hand side of Eq. (24) must incorporate the production and loss terms $\{P_i\}$ and $\{L_i\}$. A proper physical interpretation of 1-D ozone effects is then very difficult, because such results are based on global-annual ensemble averages of not only the atmospheric transports but also of the photochemistry and shortwave solar radiation (or solar zenith angle), chemical kinetics, heterogeneous chemistry and emissions of aircraft engine effluents. However, the common practice of using 1-D photochemical models to forecast anthropogenic ozone effects motivates interest in exploring the characteristics of 1-D transport coefficients in the critical region of the lower stratosphere and upper troposphere for such effects. This can again be done by using 3-D GCM/tracer model data, i.e., by obtaining estimators from the 1-D global-annual average of 3-D GCM/tracer data for the vertical fluxes and vertical gradients of mixing ratio as required by, say, Eq. (23) with $R_1 = R$ for a chemically inert tracer.

Recent results from numerical experiments at the Geophysical Fluid Dynamics Laboratory allow a rather comprehensive display of the characteristics of 1-D transport coefficients as a function of (1) tracer configuration in the stratosphere with regard to both the space and time (years) domains and (2) tracer-source location in the stratosphere as well as at the earth's surface. In addition to the three numerical experiments described previously, there are two more recent experiments. One is called "simple ozone", which is a refinement of the "vertical stratification" experiment for a tracer-source in the upper stratosphere. In this subsequent experiment, use was made of "simple" chemistry at the top of the model together with an instantaneous relaxation to a specified observed average ozone value at 10 mbar, but with otherwise the same inert and heterogeneous tracer characteristics as in the "vertical stratification" experiment (Mahlman, Levy, and Moxim, 1979). The other recent numerical experiment used a

small uniform source of N_2O (15 M ton/year) at the earth's surface (Levy, Mahlman, and Moxim, 1979) and is of direct interest to the CFM problem; because as CFMs, N_2O propagates upwards from the earth's surface to the stratosphere after a long residence time (several decades) in the troposphere.

Some characteristics of monthly-annual estimators for 1-D transport coefficients based on early "stratification" and "mid-latitude point source" results have been given by Mahlman (1975). These results indicated that the $K_z(z)$ profiles were not unique, i.e., the 1-D transport coefficient was found to be strongly dependent upon the tracer configuration in the stratosphere. Furthermore, these results indicated that the $K_z(z)$ profile may not necessarily be independent of time (years) as assumed in 1-D photochemical models during the transition years between the equilibrium states of an initial unpolluted to polluted stratosphere.

Table 11 shows the 1-D transport coefficients derived from the GFDL 3-D GCM/tracer model experiments as a function of

TABLE 11. 1-D TRANSPORT COEFFICIENTS $K_z(z)$, $10^4 cm^2/sec$ AS A FUNCTION OF SOURCE LOCATION AND TIME (YEARS) IN THE LOWER STRATOSPHERE AND TROPOSPHERE (Mahlman, 1980)

LEVEL	ALTITUDE*	POINT-SOURCE		LINE-SOURCE		STRATIFICATION		"SIMPLE O_3"	N_2O
(mbar)	(km)	Year 1	Year 4	Year 7	Year 9	Year 1	Year 4	Year 4	**
27.6	24.2	8.44	1.49	2.43	-2.16	0.52	0.74	0.60	1.21
52.3	20.2	0.10	0.77	1.99	-2.36	0.42	0.61	0.66	0.62
80.7	17.6	0.65	1.26	1.26	1.41	0.92	1.10	1.14	1.01
149.9	13.7	1.92	1.25	1.86	1.92	1.52	1.11	1.16	0.84
240.6	10.5	7.02	3.67	12.94	13.00	5.19	3.91	3.94	10.77
412.0	6.8	9.53	6.24	11.54	11.61	12.53	6.00	6.13	9.57
606.7	4.0	10.04	11.29	44.03	42.34	18.31	12.32	12.80	-?

*Standard altitude.

**Equilibrium conditions (reached after ~ 2000 years).

tracer-source location and tracer configuration, i.e., tracer-source characteristics and/or time (years). The results in Table 11 indicate the following:

- For the point and line sources in the lower stratosphere of interest for aircraft ozone effects, the 1-D transport coefficients for the lower stratosphere can be a function of both source characteristics and year. For example, at 20.2 km, the two instantaneous-point source columns show that the value of the 1-D transport coefficient for the first year can increase by a factor of about eight in the subsequent year; whereas the corresponding constant-line source columns indicate that the 1-D transport coefficient for the ninth year can become negative, a fact that implies distortions of the K(z) profile (Mahlman, 1980).
- The altitude for the minimum value of the 1-D transport coefficient, which is of critical importance for predictions of anthropogenic ozone effects, can be a function of source location. For example, the N_2O column indicates that the altitude for minimum K_z for N_2O is at about 13.7 km; which is lower than that (20.2 km) for the instantaneous-point source at mid-latitudes in the lower stratosphere.

Although the results in Table 11 are subject to constraints that may be introduced by the rather low vertical resolution (3 km) of the GCM/tracer model in the critical tropopause and lower stratosphere regions, the *trends* established by such extensive calculations may not be ignored in the absence of global observations involving suitable tracers for an ensemble of many years. Hence, 1-D transport coefficients that are assumed to be independent of tracer configuration (i.e., tracer-source location and characteristics as well as years) as usually done in 1-D photochemical models, cannot avoid serious distortions in their prognostic descriptions of transports.

REFERENCES

Andrews, D.G. and M.E. McIntyre, "An Exact Theory of Non-Linear Waves on a Lagrangian-Mean Flow," *J. Fluid Mech.*, Vol. *89*, pp. 609-646, 1978a.

Andrews, D.G. and M.E. McIntyre, "On Wave Action and Its Relatives," *J. Fluid Mech.*, Vol. *89*, pp. 647-664, 1978b.

Andrews, D.G. and M.E. McIntyre, "Planetary Waves in Horizontal and Vertical Shear: The Generalized Eliassen-Palm Relation and the Mean Zonal Acceleration," *J. Atmos. Sci.*, Vol. *33*, No. 11, pp. 2031-3048, November 1976.

Broderick, A., "Stratospheric Effects from Aviation," Presented at AIAA/SAE 13th Propulsion Conference, Orlando, Florida, July 11-13, 1977, U.S. Department of Transportation, Federal Aviation Administration, AIAA Preprint No. 77-799, 1977.

Clark, J.H.E. and T.G. Rogers, "The Transport of Trace Gases by Planetary Waves," *J. Atmos. Sci.*, Vol. *35*, pp. 2232-2235, 1978.

Crutzen, P.J. (1980): Private communication.

Crutzen, P.J., I.S. Isaksen, and J.R. McAfee, "The Impact of the Chlorocarbon Industry on the Ozone Layer," *J. Geophys. Res.*, Vol. *83*, January 20, 1978.

Danielsen, E.F. and J.F. Louis, "Transport in the Stratosphere," *The Upper Atmosphere and Magnetosphere (Studies in Geophysics)*, Geophysics Study Committee, National Research Council, National Academy of Sciences, Washington, D.C., 1975.

Dunkerton, T., "On the Mean Meridional Mass Motions of the Stratosphere and Mesosphere," *J. Atmos. Sci.*, Vol. *35*, pp. 2325-2333, 1978.

Grobecker, A.J., S.C. Coroniti and R.H. Cannon, Jr., *Report of Findings--The Effect of Stratospheric Pollution by Aircraft*, DOT-TST-75-50, prepared by the Department of Transportation, CIAP, December 1974.

Hidalgo, H., *Status of Representative Two-Dimensional Models of the Stratosphere and Troposphere as of Mid-1978*, Report No. FAA-AEE-78-23, U.S. Department of Transportation, Federal Aviation Administration, Office of Environment and Energy, Washington, D.C., October 1978.

Hidalgo, H. and P.J. Crutzen, "The Tropospheric and Stratospheric Composition Perturbed by NO_x Emissions of High Altitude Aircraft," *J. Geophys. Res.*, Vol. *82*, No. 37, pp. 5833-5866, December 20, 1977.

Holloway, J.L., Jr. and S. Manabe, "Simulation of Climate by a Global General Circulation Model: 1. Hydrolic Cycle and Heat Balance," *Mon. Wea. Rev.*, Vol. *99*, pp. 335-370, 1971.

Holton, J.R., "The Dynamic Meteorology of the Stratosphere and Mesosphere," *Meteorol. Mono.*, Vol. *15*, No. 37, August 1975.

Holton, J.R. (1980): Private communication.

Levy II, H., J.D. Mahlman, and W.J. Moxim, "A Preliminary Report on the Numerical Simulation of the Three-Dimensional Structure and Variability of Atmospheric N_2O," *Geophys. Res. Lett.*, Vol. *6*, No. 3, pp. 155-158, 1979.

Lorenz, E.N., *The Nature and Theory of the General Circulation of the Atmosphere*, World Meteorological Organization, WMO No. 218, TP 115, 1967.

Louis, J.F., *A Two-Dimensional Transport Model of the Atmosphere*, Ph.D. Dissertation, University of Colorado, Boulder, Colorado, 1974.

Luther, F.M., *Monthly Values of Eddy Diffusion Coefficients in the Lower Stratosphere*, UCRL Report 74616. Also AIAA Paper No. 73-498, AIAA/AMS International Conference on the Environmental Impact of Aerospace Operations in the High Atmosphere, Denver, Colorado, June 1973.

Mahlman, J.D., "A Three-Dimensional Test of One-Dimensional Eddy Diffusion Theory, *Geophys. Res. Lett.*, to be submitted 1980.

Mahlman, J.D. (1978, 1979): Private communications.

Mahlman, J.D., "Some Fundamental Limitations of Simplified Transport Models as Implied by Results from a Three-Dimensional General Circulation/Tracer Model, *Proceedings of the Fourth Conference on the Climatic Impact Assessment Program*, February 4-7, 1975, edited by T.M. Hard and A.J. Broderick, U.S. Department of Transportation, DOT-TSC-OST-75-38, pp. 132-146, 1975.

Mahlman, J.D., H. Levy II, and W.J. Moxim, "Three-Dimensional Tracer Structure and Behavior as Simulated in Two Ozone Precursor Experiments," *Geophys. Res. Lett.*, pp. 155-158, 1979.

Mahlman, J.D. and W.J. Moxim, "Tracer Simulation Using a Global General Circulation Model: Results from a Mid-Latitude Instantaneous Source Experiment," *J. Atmos. Sci.*, Vol. *35*, No. 8, pp. 1340-1374, 1978.

Mahlman, J.D., "Preliminary Results from a Three-Dimensional General Circulation/Tracer Model," *Proceedings of the Second Conference on the Climatic Impact Assessment Program,* November 14-17, 1972, edited by A.J. Broderick, U.S. Department of Transportation, DOT-TSC-OST-73-4, pp. 321-337, April 1973a.

Mahlman, J.D., "A Three-Dimensional Stratospheric Point-Source Experiment and Its Implications for Dispersion of Effluents from a Fleet of Supersonic Aircraft," Presented at the *AIAA/AMS International Conference on the Environmental Impact of the Aerospace Operations in the High Atmosphere,* AIAA Paper 73-528, Denver, Colorado, June 1973b.

Manabe, S. and J.D. Mahlman, "Simulation of Seasonal and Interhemispheric Variations in the Stratospheric Circulation," *J. Atmos. Sci.*, Vol. *33*, 1976.

Manabe, S. and J.L. Holloway, Jr., "The Seasonal Variation of the Hydrological Cycle as Simualted by a Global Model of the Atmosphere," *J. Geophys. Res.*, Vol. *80*, pp. 1617-1649, 1975.

Matsuno, T., "Lagrangian Motion of Air Parcels in the Stratosphere in the Presence of Planetary Waves," Geophysical Institute, University of Tokyo, March 1979, submitted to *PAGEOPH,* 1980.

NASA Reference Publication 1010, "Chlorofluoromethanes and the Stratosphere," edited by R.D. Hudson, August 1977.

National Academy of Sciences, *Halocarbons: Effects on Stratospheric Ozone,* Panel on Atmospheric Chemistry, National Research Council, 1976.

National Academy of Sciences, *Environmental Effects on Chlorofluoromethane Release,* Committee on Impact of Stratospheric Change, National Research Council, 1976.

National Academy of Sciences, *Environmental Impact of Stratospheric Flight, Biological and Climatic Effects of Aircraft Emissions in the Stratosphere,* Climatic Impact Committee, 1975.

Oliver, R.C., E. Bauer, H. Hidalgo, K.A. Gardner and W. Wasylkiwskyj, *Aircraft Emissions: Potential Effects on Ozone and Climate,* Prepared for High Altitude Pollution Program, FAA-EQ-77-3, U.S. Department of Transportation, Federal Aviation Administration, March 1977.

Oört, A.H. and E.M. Rasmusson, *Atmospheric Circulation Statistics,* NOAA Professional Paper 5, Geophysical Fluid Dynamics Laboratory, Princeton University, Princeton, New Jersey, 1971.

Plumb, R.A., "Eddy Fluxes of Conservative Quantities by Small-Amplitude Waves," *J. Atmos. Sci.*, Vol. *36*, pp. 1699-1721, 1979.

Prandtl, L., "Über die ausgeleildete Turbulenz," *Zamm*, Vol. *5*, No. 136, 1925 and Proceedings of II International Congress of Applied Mechanics, Zürich, 1926.

Reed, R.J. and K.E. German, "A Contribution to the Problem of Stratospheric Diffusion by Large Scale Mixing," *Mon. Wea. Rev.*, Vol. *93*, May 1965.

Wallace, J.M., "Trajectory Slopes, Countergradient Heat Fluxes and Mixing by Lower Stratospheric Waves," *J. Atmos. Sci.*, Vol. *35*, pp. 554-558, 1978.

Widhopf, G.E. (1978): Private communication.

Widhopf, G.E., L. Glatt, and R.F. Kramer, "Potential Ozone Column Increase Resulting from Subsonic and Supersonic Aircraft NO_x Emissions," *AIAA Journal*, Vol. *15*, No. 9, pp. 1322-1330, September 1977.

APPENDIX

This Appendix provides the sample GFDL/GCM data for a 6-hour period as a function of latitude, pressure level, and longitude. The data shows the vertical (w), northward (v), and eastward (u) winds in cm/sec at 28°N, 48°N, and 72°N latitude. Note that the number of longitudinal points decrease from 138 at the lowest latitude to 99 and 45 at the middle and high latitudes, respectively. This Appendix also gives a computer program for the calculation of the $[\alpha]$ and $[\alpha^{*2}]$ statistics based on both the Reed and German definition (Eq. 14) and by replacing arbitrarily the northward wind by the eastward wind. The former slope is denoted by α_1, and the latter by α_2. The purpose of computing α_2 was to investigate if the $[\alpha_1]$ and $[\alpha_1^{*2}]$ undeterminability of the statistics would be modified from possible consideration of the zonal circulation. The results were negative, i.e., the undeterminability of $[\alpha_2]$ and $[\alpha_2{}^*]$ was as that of the Reed and German $[\alpha_1]$ and $[\alpha_1{}^{*2}]$.

TABLE A-1. W-VERTICAL WIND, LATITUDE 24 DEGREES NORTH

PRESSURE LEVEL

38MB	65MB	110MB	190MB
-1.172	-3.969	.700	1.270
-1.077	.186	.459	1.149
.218	.286	-.340	.814
.089	-.834	-.519	1.470
.823	.814	-1.230	-2.198
.606	.891	-1.041	-2.436
.515	-1.144	-.495	-5.157
1.303	-1.201	-.475	-1.131
.999	-2.179	-.701	1.663
.968	-1.141	-1.576	.602
.475	.641	-1.835	-.965
1.297	1.925	-1.600	-3.593
.573	1.570	-.256	-.128
-.578	1.918	-.047	-.282
-1.634	-.799	1.321	.697
-1.830	-1.237	2.638	1.380
.290	-1.843	-1.296	-.188
2.005	-1.098	-1.711	.674
2.679	.559	-2.288	-.146
1.470	-.906	.006	-2.817
.277	-.061	1.974	-1.325
1.297	-1.581	-.006	3.635
.777	-1.676	-.821	5.422
-.128	-.179	.781	3.304
.054	2.456	-1.007	-1.397
-1.072	4.337	.408	-2.327
-1.858	1.150	3.814	2.796
-.274	-1.863	1.859	4.367
-.896	1.422	.176	3.267
.415	-.582	1.915	2.997
.723	.914	-.103	-.728
-.368	2.690	-2.146	-3.094
-2.395	.340	4.200	-1.397
-.936	-2.270	3.246	3.741
.829	-2.764	-1.922	.803
.619	-2.036	-3.101	-3.314
-.688	-1.112	-1.931	-1.610
-1.577	.636	2.608	3.105
-.605	-1.409	-.753	-1.581
-.609	-1.996	-.014	.692
-.843	-1.138	1.989	5.780
.558	-1.470	1.252	2.972
-.129	-2.190	1.260	4.857
.819	-.021	-2.637	7.059
-.214	-.463	1.533	4.676
-2.063	-2.403	4.080	2.510

TABLE A-1. CONTINUED

38MB	65MB	110MB	190MB
-.551	-.916	.273	-.676
.657	1.447	-.933	-5.222
-.240	-1.052	2.659	-1.624
.823	-2.830	2.404	-.428
.047	-1.007	2.127	-.241
-.550	.392	2.138	-2.846
1.340	.147	.804	-2.114
.844	1.151	2.058	.242
.738	-.868	1.405	4.270
.579	-2.043	2.355	6.069
.472	-2.124	-.683	2.798
.567	.034	.030	-5.305
1.015	-1.640	4.122	-2.499
1.006	.331	3.828	-1.521
.795	1.652	1.626	-.849
1.413	2.554	1.938	-1.548
.666	-.022	2.056	-1.136
.218	.224	1.692	-2.229
-.159	1.706	1.786	-1.846
-1.571	2.701	2.168	-1.098
-2.628	.670	.358	3.444
-2.489	-2.713	-.241	6.545
-1.753	-4.412	-2.228	2.387
-.966	-4.773	-2.156	-1.328
.524	-2.938	-2.411	-5.179
1.295	-3.060	-3.827	-3.213
.597	-2.846	-2.592	-.444
-.403	1.735	-2.899	-4.266
-.375	3.947	-4.628	-6.360
-.717	.783	-2.803	-3.737
-.678	-1.552	-1.210	-2.634
.398	.060	-.237	-1.783
.825	-.389	-3.485	-3.310
-1.743	-.661	.583	-.116
.483	.974	-.603	-4.364
-1.911	-2.910	.044	.992
-1.886	-.533	2.391	.120
-.045	.005	-.002	-4.733
-.435	.264	.967	-.332
-.716	-2.579	-.840	-.009
-1.587	.874	.239	-.901
-1.287	.821	.146	-1.993
.229	-1.630	-1.304	2.125
-.154	-.329	-.520	1.331
.617	-1.221	-.004	-1.844
.200	-.932	-.538	-1.314
-.679	2.342	.168	-1.268

TABLE A-1. CONTINUED

30MB	65MB	110MB	190MB
.080	-.249	-.012	-.474
-1.427	-1.182	.395	-.546
-.284	-1.597	1.029	-.026
-.893	-.888	1.302	-2.959
.250	2.066	.274	3.505
1.348	1.851	.230	-.866
.495	.692	-.203	-5.607
-.300	1.245	-1.643	.115
-.848	2.314	.108	-2.242
-.467	.180	1.201	.386
.679	-1.044	.902	1.394
-.280	-1.399	.742	1.855
.548	-.535	-.259	2.456
-.383	.865	.116	2.853
-.489	.640	-.274	3.385
1.108	-.675	-.443	1.101
.592	-.604	-.843	2.756
.849	2.325	-.718	-2.177
.032	-2.710	1.815	-2.804
-.265	-.627	1.796	-1.801
1.633	-1.199	-1.402	2.594
-.315	1.274	-.719	2.901
-1.518	3.076	.996	-1.892
-.941	3.056	.518	-6.743
-.661	2.298	1.145	-3.982
1.793	-4.817	-2.993	6.337
2.224	-2.277	-4.672	1.069
.381	3.080	-.842	-3.480
-.412	-1.828	-.228	-.291
.577	-.768	.208	-.833
-.123	-2.531	-.748	2.626
1.299	-1.964	-2.491	1.843
-1.027	-.715	.134	.614
-.029	-.914	-.303	-.250
.374	-1.161	-.976	-.267
-.488	.073	.827	-.165
.525	-.888	-.284	-.643
.187	1.530	-.187	-1.255
.316	.539	-.314	-.194
.802	.965	-.695	-2.118
.874	-.322	.376	-.137
-.463	.145	1.092	-.776
.480	2.643	.398	-1.537
-.112	-1.914	-1.273	2.294
-.442	-2.896	1.024	1.367

TABLE A-2. V-NORTHWARD WIND, LATITUDE 24 DEGREES NORTH

PRESSURE LEVEL

30MB	60MB	110MB	190MB
-329.046	262.474	327.525	1117.362
-401.086	-2.031	811.803	782.038
-494.069	-71.610	379.899	838.737
-322.767	-4.822	245.617	658.946
-68.487	-251.413	-252.442	274.266
-45.870	-383.344	-531.673	334.365
215.221	-311.136	-268.055	-143.699
313.971	-501.561	-674.612	-62.151
509.334	-72.071	-691.783	-220.715
635.894	-272.349	-339.756	-480.911
725.267	-447.180	-133.749	-261.330
507.846	-366.391	-132.787	-383.004
654.181	-192.572	-18.049	-150.720
700.206	-206.810	-302.234	-200.472
949.595	-202.280	-164.709	8.319
71.073	64.456	110.267	150.060
92.209	573.974	12.522	-186.367
846.057	748.472	282.799	250.758
666.144	814.519	401.616	442.094
336.899	770.485	480.029	300.685
155.907	464.886	614.020	177.635
297.336	161.936	213.788	152.409
770.466	493.643	59.439	-94.864
411.997	893.913	409.600	-149.976
305.974	672.726	779.654	40.992
355.164	424.879	829.310	-206.111
-120.116	311.521	419.082	-190.843
52.016	310.302	808.049	-319.811
122.213	184.353	809.916	67.804
526.200	138.102	265.097	-48.934
431.178	258.824	115.721	201.416
-205.456	-869.161	760.854	430.246
-260.353	-61.911	599.607	1089.567
-586.355	-60.543	511.109	1240.001
197.981	-1198.348	316.214	1223.987
-193.219	-990.405	937.012	1642.629
-432.573	-1658.425	101.390	1360.172
-703.993	-242.083	56.118	1131.915
-66.771	127.660	-421.088	889.275
-49.996	150.216	-219.135	651.750
-170.371	429.917	324.119	1153.464
-103.365	730.468	-1035.940	460.057
139.913	-119.508	203.173	95.677
44.841	82.107	-230.302	-569.307
696.254	372.576	350.070	189.704
136.288	873.848	328.807	-112.373

TABLE A-2. CONTINUED

30MB	65MB	110MB	190MB
215.378	1160.386	482.883	-174.195
481.010	262.103	638.443	288.006
529.043	756.032	1628.848	742.403
198.875	927.805	1836.862	1312.361
649.337	1111.728	874.571	769.146
486.683	991.822	1582.330	553.552
964.373	1134.634	1813.171	2005.783
727.986	1103.003	1653.610	1647.380
1172.241	1256.426	1515.958	2081.016
1101.034	1381.063	1403.804	1343.161
1435.823	1234.011	1609.210	1592.804
1460.263	423.109	1621.606	1939.033
1524.400	573.718	2292.775	1643.738
1260.246	274.949	2298.725	1170.612
1123.259	893.134	1490.539	718.467
878.098	731.271	1287.843	832.804
963.691	227.562	825.301	517.101
704.661	187.736	413.805	159.510
437.020	259.428	432.560	-326.162
104.870	210.089	229.772	-482.301
-150.680	7.643	-319.207	-473.678
-108.451	-366.538	-774.380	-358.476
-224.616	-753.324	-1436.833	-531.739
-227.347	-858.162	-1763.741	-1490.726
64.448	-944.121	-1933.951	-2278.510
-26.337	-982.499	-2108.452	-2727.109
80.169	-732.602	-1679.149	-3061.310
-174.903	-286.675	-1708.373	-3383.873
-156.981	37.561	-2117.418	-3572.242
-436.256	-631.696	-2207.658	-2871.008
-302.084	-272.755	-2079.202	-2424.986
-353.831	-576.419	-1724.082	-1881.806
-335.678	-779.482	-918.147	-1250.013
-611.891	-1123.935	-1005.731	-998.654
-798.134	-759.436	-992.898	-1071.767
-864.586	-1429.421	-786.198	241.812
-867.549	-622.079	-568.304	-375.492
-819.921	-754.824	-522.024	-969.454
-891.870	-416.805	-573.507	-859.955
-1227.743	-386.840	-666.409	-860.368
-1041.928	-424.707	-874.808	-1095.280
-1270.310	-455.830	-375.424	-708.898
-983.089	-517.508	-155.035	-160.159
-1001.347	-599.164	270.687	707.680
-668.778	-656.292	318.855	574.092
-850.829	-458.620	133.441	580.389
-442.580	-227.359	408.773	543.517

TABLE A-2. CONTINUED

38MB	65MB	110MB	190MB
-530.392	-376.301	315.558	813.332
-597.411	-421.611	51.329	987.462
-632.890	345.978	-97.250	-198.605
-1554.198	-118.677	427.956	1183.926
-1390.850	4.234	225.059	-663.930
-1075.595	495.424	443.779	856.644
-883.251	97.293	742.305	1299.240
477.795	823.029	268.393	-539.116
190.664	-635.069	438.433	139.220
47.797	10.191	-77.794	-735.253
42.057	-186.794	5.791	-415.112
242.369	10.928	-594.967	-855.865
52.161	815.074	-246.503	-1051.417
171.787	396.494	-250.469	-935.446
150.934	470.617	-63.522	-699.494
207.562	327.134	248.109	144.312
156.367	379.182	824.243	372.226
301.527	-169.914	839.413	574.958
182.410	-96.680	61.550	929.166
56.689	-148.852	185.229	744.842
-38.574	-83.864	298.544	-170.882
79.983	-456.957	108.544	-336.110
480.072	-588.137	-24.836	-519.938
250.014	-474.076	-637.283	141.828
241.592	-257.034	-570.513	-109.868
-74.335	521.168	-1065.978	-748.526
-467.517	272.592	-629.164	-522.459
-26.964	-734.509	-503.904	-627.687
624.881	-346.117	-686.798	-815.709
-252.210	-311.007	-348.396	-348.915
36.678	-311.024	-440.726	-603.188
-336.440	-200.950	-173.510	-382.241
-214.475	-240.189	-580.531	-490.995
-481.920	-86.110	-429.453	-529.746
-363.938	-82.399	-441.214	-470.834
-639.884	-222.406	-164.671	-266.553
-460.471	-8.234	-172.133	-83.427
-589.835	271.267	453.846	219.674
-235.836	-178.981	341.119	148.217
-304.838	242.752	562.739	380.023
-114.657	298.018	473.490	552.487
-317.729	779.274	362.682	608.997
-353.338	548.067	881.481	790.029
-311.884	288.788	761.003	538.195
-624.444	781.488	569.089	1063.007

TABLE A-3. U-EASTWARD WIND, LATITUDE 24 DEGREES NORTH

PRESSURE LEVEL

30MB	65MB	110MB	190MB
384.598	1834.420	2417.166	3152.145
1084.992	1830.299	2827.986	3332.916
903.213	1184.909	2653.702	3242.558
1135.485	1435.065	2808.803	3616.870
1087.533	1309.434	2740.865	3558.456
1169.189	1338.840	2947.891	3955.007
1307.868	1172.967	3035.335	3892.459
1378.567	939.596	3430.700	4385.387
1511.145	1420.577	2946.295	4287.051
1250.673	1889.272	2968.383	4646.441
1255.164	1808.208	3013.409	4185.016
779.873	1869.748	3340.832	4700.359
613.037	1859.598	3825.912	4437.738
224.330	1554.819	3458.319	4640.809
632.046	1738.997	3420.010	4182.043
388.610	799.529	3003.582	4237.703
283.078	862.108	3165.354	4359.398
191.606	1006.614	2851.450	3691.066
-428.619	800.407	3148.780	3866.260
-359.884	911.327	3133.782	3471.464
-589.856	591.596	3112.258	3735.254
-755.243	618.397	3403.320	4019.003
-1708.440	807.196	2913.055	3962.871
-1020.615	488.607	2464.234	3954.128
-1626.974	628.292	2657.494	4133.254
-1714.341	603.573	3167.803	4047.441
-1588.347	132.864	3517.686	4310.312
-1635.057	153.278	3189.936	4287.965
-1451.186	205.519	3414.677	4495.344
-926.880	-.158	3313.930	4431.121
-1144.247	403.411	3020.665	4633.375
-1028.466	414.381	3473.574	4514.324
-562.525	724.165	3591.531	4009.144
-382.014	678.409	3644.781	5182.820
-191.651	621.876	2727.414	4345.355
-655.149	1062.183	3504.617	5011.031
-188.975	1758.395	3278.491	4531.199
-184.033	1614.700	3610.302	4498.016
-947.390	718.688	2878.739	4410.426
-858.430	638.193	2736.694	4908.941
140.882	434.288	1649.389	4152.477
-418.214	271.651	2131.850	4504.246
-672.448	638.487	1548.604	4509.133
-721.638	493.836	2498.319	4218.465
-1058.054	747.309	2475.721	3884.131
-1077.342	632.823	2475.290	4277.488

TABLE A-3. CONTINUED

38MB	65MB	110MB	190MB
-1086.887	604.201	2373.991	3966.291
-1311.998	264.450	2446.659	3376.459
-1395.987	274.643	2635.112	3005.099
-1457.267	50.284	2074.744	2625.135
-1581.714	409.914	1604.935	2051.600
-1620.328	8.827	1159.909	1275.570
-1414.626	187.893	1314.617	1296.887
-1949.380	-484.326	1392.211	1581.656
-1943.627	-559.116	1592.368	1511.708
-2225.904	-679.505	1239.547	1419.325
-1927.631	-519.329	509.808	1335.580
-1886.593	-624.115	816.707	878.980
-1880.571	-824.281	976.118	531.250
-2075.076	-1061.789	35.597	840.453
-1981.915	-1346.452	-428.844	927.761
-2597.520	-1531.280	-9.590	738.347
-2752.719	-1513.957	-96.797	982.937
-3037.968	-1537.590	-287.496	902.434
-3120.718	-1787.325	-588.986	814.195
-3324.514	-1862.336	-423.179	488.614
-3324.570	-2338.493	-418.279	869.638
-3036.251	-2339.428	-706.593	667.006
-2988.394	-2648.379	-819.607	268.392
-2423.587	-2472.834	-1123.209	-101.896
-2439.974	-2402.503	-1319.181	53.442
-2418.363	-1889.631	-976.559	252.718
-2690.259	-1102.809	-535.955	530.541
-2557.384	-717.554	-762.918	578.468
-2624.131	-1017.556	-137.004	217.871
-2692.858	-1406.917	107.715	579.036
-2727.531	-1348.019	132.810	651.457
-2857.497	-1453.164	75.806	1222.507
-3210.073	-938.550	397.726	1531.797
-2989.591	-1114.093	800.992	1734.585
-3193.958	-1032.162	497.980	1853.473
-3252.159	-876.193	1004.992	1716.240
-2786.698	-887.785	640.184	1361.948
-3026.691	-634.912	881.826	1820.519
-2886.697	-718.462	1159.208	1848.618
-2729.185	-464.868	911.987	1809.693
-2647.191	-198.352	1105.221	1989.088
-2420.390	-583.560	1028.036	1715.785
-2466.554	-262.583	1471.232	1959.838
-2286.924	-102.526	1022.481	1101.738
-2091.875	38.827	1564.748	1880.509
-1886.958	479.386	1251.997	1787.148
-1585.871	438.125	1488.243	1849.678

TABLE A-3. CONTINUED

PHESSURE LEVEL

38MB	65MB	110MB	190MB
-1465.428	230.849	1268.442	684.915
-1043.990	524.230	1395.057	1503.412
-764.520	807.479	1576.761	1256.561
-549.097	778.438	1277.236	2252.164
-471.841	1210.765	1470.130	1823.163
-219.681	962.086	2053.316	2309.148
648.339	1700.619	2106.404	2352.089
-333.843	810.614	1887.181	3057.763
191.410	868.815	2148.289	2322.461
145.249	344.396	2190.600	2685.757
446.167	766.708	2170.538	2546.930
402.032	711.948	2310.096	3115.415
897.796	1120.417	2035.633	3330.645
424.484	1160.806	2215.586	3579.276
989.110	777.897	2147.096	3365.855
510.820	874.008	2332.413	3308.018
645.298	1062.691	1873.984	3354.058
768.640	836.591	2396.409	2676.079
667.372	640.342	2382.856	2482.479
814.930	770.847	1810.836	2945.897
534.639	910.730	1757.469	2731.576
250.050	1476.687	1677.591	2221.167
854.821	693.075	2118.921	1696.089
1091.715	450.942	2245.607	2172.740
1209.950	216.697	2546.409	2352.817
1147.067	510.984	2273.065	2599.513
808.790	1671.354	1685.590	1948.804
493.636	1288.912	2305.820	2072.056
1042.228	780.458	2222.197	1741.511
860.067	1037.987	2113.397	1639.479
981.614	580.984	1740.805	1706.168
965.762	862.233	1626.909	1657.039
796.769	669.578	1645.233	1605.022
1294.281	807.779	1472.805	1726.999
775.794	460.144	1396.578	1665.252
1050.087	432.689	1488.786	1746.046
697.743	171.773	1321.837	1817.289
806.015	564.317	1532.076	1994.728
323.865	450.266	1824.265	1869.146
870.883	290.616	2011.670	2056.712
81.962	643.873	2318.023	2245.712
215.974	934.627	2074.418	2449.041
207.752	1212.566	2635.473	2929.778
112.812	1134.411	2733.474	2849.670
494.161	1570.221	3173.588	2781.895

TABLE A-4. W-VERTI[illegible] OF 48 DEGREES NORTH

30MB	60MB	[illegible]MB	190MB
1.636	.925	.551	.730
.982	.98[illegible]	.360	-.308
1.695	1.394	.498	-.139
1.332	-1.090	-.010	-.411
1.206	.015	-.001	-1.047
1.211	2.043	1.214	-.478
1.899	2.298	1.090	.590
2.567	1.775	-.130	1.648
3.178	-2.073	-1.034	1.288
.549	-1.480	.748	.548
.055	.412	.486	.572
.078	-.388	.483	.617
-1.023	2.845	.699	-1.348
.372	2.621	-.020	-1.472
2.763	-2.515	-2.231	.129
-.285	-.840	-.811	-.107
-1.936	1.073	.922	-1.852
.539	.152	-1.692	.128
.494	-1.225	-1.516	1.192
.895	-1.246	-.712	-1.465
1.417	-1.408	-.678	-1.078
.210	1.200	.136	-1.055
-.859	2.445	1.679	-.737
1.608	.872	.668	.541
1.698	-1.475	.592	.086
1.849	-.123	.879	.040
4.418	6.217	2.113	-.071
3.901	3.908	1.046	.705
2.734	4.129	3.031	.756
4.114	6.266	4.204	2.618
5.860	4.905	1.769	3.186
4.001	.466	-.020	2.320
2.070	.319	1.413	.747
1.596	.470	1.601	1.353
1.128	2.708	1.795	1.081
1.368	1.439	1.197	1.466
2.390	-.939	.278	1.731
-.553	.475	1.632	.762
-.368	1.947	.630	-.246
2.718	6.053	-.022	.446
1.972	2.056	.093	1.460
-.261	-1.911	.897	1.880
-.282	-.501	1.795	.673
.960	-1.441	.695	.521
1.437	-.412	.982	.016
-.048	1.584	1.816	.912
.579	1.973	.894	1.703
.619	1.074	-1.413	1.986
1.687	-.315	-1.821	2.109

TABLE A-4. CONTINUED

38MB	65MB	110MB	190MB
.719	.917	1.019	-.838
-2.577	2.797	5.358	-2.899
-2.551	-.469	3.635	-1.727
1.035	-1.501	-1.581	-.720
.473	2.543	-.242	.049
-2.126	.620	.897	-.749
-1.817	-.485	.724	-1.667
-.830	-.990	-.553	-.985
-.631	-.988	-1.110	-.374
-.991	-1.817	-1.197	-.069
.191	.524	-.699	-1.617
-1.638	-2.515	-2.300	-.910
-1.310	-3.223	-4.162	.224
-.935	.248	-2.191	-2.444
-3.531	-3.571	-.756	-2.480
-3.780	-5.560	-1.857	-1.224
-2.799	-.697	-2.558	-3.245
-1.897	-1.686	-3.113	-3.640
-2.389	-1.857	-1.485	-2.546
-4.774	-3.409	-.342	1.082
-3.030	-4.259	-2.734	.583
-1.596	-3.518	-2.032	.342
-4.474	-4.419	-.955	1.774
-3.024	-.214	.500	-.560
-1.833	.011	-1.040	-1.539
-.422	-1.619	-2.291	-.930
-1.247	-2.868	-.166	-1.606
-2.619	-2.664	1.576	-1.315
-2.447	-.022	1.419	1.155
-2.410	.585	-.493	1.164
-1.556	-1.702	-1.981	-.988
-3.159	-3.372	-3.020	-2.259
-3.342	-.171	-2.098	-4.056
-5.050	-3.160	-1.155	-1.986
-3.060	-5.678	-2.203	-.305
-.600	-3.044	-3.609	-1.218
-.114	.005	-2.464	-1.827
-1.295	-.746	-.951	-1.791
-1.497	-.948	.516	-.547
-1.311	.454	.773	-.105
1.025	2.024	.847	-.564
1.682	2.582	1.582	-.137
2.233	2.916	2.260	.423
2.100	3.357	2.693	1.125
1.447	2.683	2.427	1.374
1.381	3.565	2.655	1.770
2.640	4.089	1.502	.827
2.666	3.136	1.400	.782
1.757	.721	.705	.206
1.237	2.056	1.708	.859

TABLE A-5. V-NORTHWARD WIND, LATITUDE 48 DEGREES NORTH

PRESSURE LEVEL

38MB	65MB	110MB	190MB
-604.411	-837.265	-712.526	-385.742
-486.752	-874.426	-193.797	-81.441
-613.083	-592.487	-403.736	-261.201
-343.640	-413.764	-145.310	321.135
-704.730	-478.894	-230.606	295.078
-491.703	-619.666	-523.582	-418.697
-141.254	-648.543	-904.210	-1481.890
-557.107	-6.477	-771.458	-1620.387
-36.083	308.097	-901.899	-844.254
301.835	-130.513	-436.404	-361.989
205.650	-183.427	143.989	-45.113
867.365	-178.153	394.569	213.397
724.355	-294.794	772.404	469.396
501.280	748.254	677.145	513.153
445.073	1464.761	397.128	1176.887
1375.282	596.829	687.935	848.087
1448.500	396.449	1161.358	444.848
1084.148	518.149	774.142	923.960
961.462	1031.458	638.704	821.307
478.212	593.684	519.524	1113.553
451.066	414.513	460.374	1105.219
80.126	-133.149	452.216	696.087
-265.445	-172.806	357.273	691.907
-366.325	-67.598	315.173	753.271
38.303	-26.723	59.921	179.460
-102.392	-486.804	-635.986	-557.694
-104.136	-1054.954	-1117.995	-1516.417
-125.860	-1033.493	-1146.983	-1785.645
-59.508	-1328.565	-1943.244	-2660.673
-111.079	-1176.732	-1942.790	-3078.460
-255.376	-478.387	-1967.009	-2876.848
353.203	-351.729	-1571.502	-1719.837
671.149	-530.787	-1064.823	-984.758
850.483	37.955	-699.806	-979.056
1053.009	-124.761	-305.487	-811.890
1391.323	680.576	130.373	-424.251
1179.389	1280.971	249.970	-94.076
1673.922	1353.378	746.493	288.912
1887.403	1677.170	1205.149	598.889
1860.992	2288.720	1702.496	619.348
2089.671	2594.137	1608.974	704.371
2197.867	1910.204	1248.902	1220.798
2383.460	1836.873	1556.906	1697.694
2093.085	1349.053	1492.023	1500.282
2228.444	1023.354	1650.144	1500.337
1716.355	552.318	1342.116	1101.839
1434.292	690.409	845.474	641.108
952.845	1143.326	582.170	-88.841
649.276	1392.466	290.590	-704.980

TABLE A-5. CONTINUED

30MB	65MB	110MB	190MB
306.429	1410.689	-107.157	-706.750
697.756	680.096	-75.651	-180.947
670.744	532.921	-216.759	386.718
452.074	472.782	-228.827	399.611
308.294	274.764	160.278	459.549
112.644	-45.462	160.632	-36.467
-137.818	386.731	32.724	-274.996
-846.277	-89.783	-131.100	-71.712
-763.742	-261.082	-261.676	-244.134
-1344.035	-577.196	-356.218	-130.052
-1572.543	-956.980	-427.145	-183.271
-1518.249	-1208.133	-327.210	219.192
-1847.635	-1129.577	-214.536	201.106
-2150.495	-1736.146	-270.804	365.473
-2517.429	-1693.208	-611.289	517.909
-2590.061	-1662.152	-494.617	887.009
-2791.149	-2073.471	-552.849	841.069
-2904.138	-1670.383	-573.942	374.017
-2992.934	-1696.555	-525.494	844.552
-2772.281	-1546.139	-855.731	-550.772
-2586.693	-1178.908	-821.046	-755.066
-2349.150	-1098.287	-875.819	-839.697
-1987.846	-1276.550	-407.401	-875.285
-1928.401	-1336.335	-55.007	-346.730
-1921.218	-526.471	-311.697	235.374
-1304.946	-19.663	-410.125	443.498
-729.391	-104.229	-619.158	327.041
-315.004	267.291	-503.456	-292.209
-130.678	224.685	-147.519	-805.198
571.842	681.687	863.492	68.313
775.181	1022.512	1283.790	1235.006
1430.146	1158.304	2087.263	2481.412
1583.210	1249.643	2328.672	2994.144
1551.650	1598.029	2103.535	2842.665
1478.863	1587.386	1682.559	2017.066
1388.911	1583.690	1621.011	1514.583
1201.544	1248.817	1546.115	1634.402
1296.712	611.140	1137.572	1403.414
1027.958	213.990	725.761	829.177
496.394	-152.527	186.306	131.206
-137.563	-432.276	-411.401	-844.442
-469.981	-641.674	-1041.028	-1701.844
-669.039	-1020.229	-1601.526	-2493.425
-685.788	-1023.134	-1609.060	-2668.814
-718.139	-953.935	-1750.004	-2347.247
-884.595	-1039.166	-1764.206	-2232.905
-876.221	-733.624	-1358.903	-1800.050
-1081.757	-574.593	-1467.429	-1283.947
-611.089	-878.585	-1060.127	-621.012
-502.657	-790.253	-1031.812	-886.612

TABLE A-6. U-EASTWARD WIND, LATITUDE 48 DEGREES NORTH

PRESSURE LEVEL

38MB	65MB	110MB	190MB
4191.051	3698.060	2202.276	1103.367
4590.578	3613.063	2469.048	1203.164
4610.937	3497.068	2707.702	1644.852
4676.773	3624.037	2698.017	1703.184
4567.973	3737.026	2840.213	2138.949
4102.500	3720.039	3046.779	2808.137
4464.246	3507.019	3177.479	3064.640
4539.383	3360.325	3057.720	2411.147
3829.212	3960.159	2910.828	2042.460
4444.664	4162.367	2506.892	2260.941
4318.840	3984.288	2716.216	2267.466
4479.746	3968.679	2882.859	2562.419
5343.664	3592.025	3065.196	2819.876
5192.047	3146.067	3698.800	3065.957
4666.723	4063.046	3565.508	3195.451
4541.629	4796.605	3342.383	3883.189
5328.898	3937.093	3647.417	3514.248
5664.203	4038.045	4127.496	3817.920
5796.195	3970.984	3629.611	3214.307
5792.355	4548.059	3781.696	3273.964
5438.625	4244.079	3371.201	3210.469
5589.297	4389.410	3373.810	2942.233
5300.789	3817.772	3188.098	2336.049
5210.258	3968.682	3146.696	2164.075
5066.730	3998.136	2837.265	1784.018
5430.945	4390.937	2713.700	1675.802
5178.340	4250.145	2702.632	1883.186
5194.062	4057.356	2933.946	1807.865
4970.293	4004.511	2909.838	2080.304
5206.766	3595.062	3057.932	2224.030
4597.023	3337.829	2992.190	1847.512
3969.970	3788.520	2625.573	1379.970
4489.582	3683.422	2455.649	1465.031
4570.273	3609.384	2328.032	1647.684
4743.359	3841.531	2014.691	1873.795
4862.469	3608.131	2792.758	1839.949
4762.070	4152.250	3078.266	2287.558
4648.430	4614.043	3532.145	2780.634
5017.059	4607.629	3868.136	3341.533
5084.031	4940.809	4525.981	3877.423
4453.500	5383.973	5162.395	3941.760
4487.566	5801.105	5339.782	4514.332
4423.422	5825.340	5365.422	4981.078
4221.031	5890.590	5785.992	5800.480
4089.597	5788.512	5980.535	6129.719
3900.795	5278.809	6451.594	6747.355
4003.517	4710.329	6379.215	6874.363
4094.741	4831.703	6483.973	7095.297
4031.332	4808.219	6244.016	6199.004

TABLE A-6. CONTINUED

38MB	65MB	110MB	190MB
3903.647	5529.008	6108.602	5379.070
3583.167	5270.957	5671.145	4875.629
4026.595	4660.937	5451.215	4866.668
4069.925	4618.082	4771.562	4743.992
4046.124	4880.117	4731.289	4581.887
3877.883	4420.738	4477.059	4183.168
4471.516	4244.258	4533.090	3970.462
4187.023	4336.910	4088.859	3553.830
4175.512	4389.691	4086.264	3403.270
4203.836	4281.105	3808.446	3184.870
3941.530	4398.672	3837.251	3067.562
3594.721	4172.734	3875.938	3005.989
4059.769	4344.008	3685.277	2638.619
4035.893	4553.273	3960.211	2420.193
4316.137	4378.559	4297.707	3030.082
4602.340	4734.349	4076.901	3014.633
5090.941	4695.387	4337.652	3758.838
5613.215	4868.437	4606.066	4215.195
5674.488	5012.781	4801.109	5041.281
5901.953	4966.129	4824.832	5891.352
6138.465	5006.133	4820.734	5492.746
6269.547	5324.344	4939.645	5789.031
6273.996	5280.406	4752.605	5188.766
6493.336	4718.258	5009.391	4698.672
6201.086	4248.277	5049.941	4170.324
5593.129	4568.576	4701.695	3570.250
5527.453	4679.996	4403.254	3587.857
5532.184	4521.254	3694.554	3661.751
5457.203	4667.590	3572.029	3646.537
5160.367	4328.359	3338.572	2996.988
5275.238	4508.262	3800.752	3219.444
5115.332	4656.281	3803.652	3484.450
5523.785	4354.569	4137.844	3744.403
5472.312	4318.305	4198.309	3444.407
5501.422	4274.786	3560.069	2927.966
5755.848	4487.031	3292.734	2615.622
5269.016	4618.305	3110.617	2199.271
5148.973	4581.551	3255.199	2374.930
5283.102	4198.781	3259.517	2902.039
5519.734	3931.562	3370.812	3408.979
5471.301	3808.622	3458.712	3589.806
5154.539	3839.253	3425.795	3564.823
4896.164	3789.275	3270.137	3283.421
4884.520	3735.028	3151.896	2784.330
4630.812	3524.256	3027.184	2353.686
4729.730	3721.554	3082.365	2465.166
4341.164	3289.562	2869.730	2287.109
4172.578	3857.905	3088.435	2201.856
3928.042	3739.401	2375.193	1798.338
4430.875	3638.027	2483.736	1649.466

TABLE A-7. W-VERTICAL WIND, LATITUDE 72 DEGREES NORTH

PRESSURE LEVEL

30MB	65MB	110MB	190MB
-.453	-.460	.219	-.364
.360	1.251	.101	-.671
-.151	.822	.201	.773
1.285	.443	.076	.022
.838	.777	.818	.435
1.031	.705	.253	.091
.941	1.314	.893	.359
.550	.128	.010	.006
.510	.129	.036	.148
.839	1.050	.828	.513
1.325	1.168	.705	.148
1.073	1.074	.742	.358
1.150	1.277	.808	.823
.411	.957	.840	.862
.186	.270	.293	.414
.168	.152	.215	.292
.365	.086	.018	.187
.323	.109	.410	.505
.683	.238	.232	.327
.777	.579	.439	.198
1.414	.680	-.417	.013
.391	.752	-.012	-.360
.179	-.117	.216	.178
-.261	.555	.382	.319
-.241	.169	-.105	.001
.971	-.593	-.713	.063
1.578	.838	.394	-.271
-.334	-.031	.067	-.167
1.159	1.202	.507	-.555
.400	1.299	.929	-.400
.490	.817	.335	-.302
.079	-.019	-.075	-.327
-.142	-.085	-.103	-.499
-.109	.172	.238	-.282
-.877	-.504	-.089	.171
-.602	-.617	.049	-.293
-.799	-.228	-.125	-.043
-.735	-.564	-.529	-.392
-.579	-.013	-.131	.756
.383	-.414	-.439	-.109
-.369	.072	-1.006	-.912
-2.808	-2.399	-.619	.174
-1.434	-.827	-.838	-1.893
-1.539	-1.701	-.771	-.944
-.548	-1.850	-.958	-.237

TABLE A-8. V-NORTHWARD WIND, LATITUDE 72 DEGREES NORTH

PRESSURE LEVEL

30MB	65MB	110MB	190MB
120.784	182.638	151.807	40.631
142.262	-18.036	-300.901	-344.986
-206.976	-435.938	-261.054	-195.428
-592.139	-788.960	-670.907	-693.366
-434.655	-424.622	-632.107	-923.878
-635.294	-650.091	-863.189	-799.626
-169.937	-858.051	-725.973	-572.424
-44.779	28.421	98.104	-110.185
108.012	289.901	111.782	-198.100
48.831	-174.670	-473.997	-579.524
-104.118	-338.847	-623.275	-741.045
-43.896	-328.919	-738.860	-778.713
-33.282	-542.402	-1004.389	-1027.062
-130.880	-438.984	-518.601	-687.767
-204.307	-278.193	-68.697	-86.589
244.138	.086	97.225	275.770
379.420	64.171	27.535	244.558
373.583	-17.678	-92.800	13.850
311.194	-228.892	-135.017	-143.821
321.879	-142.557	129.831	48.652
-83.599	-146.408	60.878	290.796
-331.752	-81.893	-144.396	-77.500
-356.090	-78.930	-105.448	-462.333
-445.598	-203.421	-356.749	-465.752
-631.854	-274.759	-76.732	225.244
-587.776	-422.525	-83.401	281.922
-909.667	-828.261	-693.804	-519.455
-1140.563	-848.261	-650.909	-650.605
-1291.974	-913.354	-908.265	-917.322
-1027.348	-1144.961	-989.008	-908.828
-968.870	-978.789	-769.585	-736.024
-602.460	-383.654	-334.215	-487.160
-280.745	-100.931	-164.589	-351.266
-20.481	188.468	291.709	90.886
732.763	763.369	1000.997	1089.244
946.677	1058.553	937.590	752.622
1193.257	1167.287	869.191	851.674
1517.582	1728.269	1461.143	1449.159
1402.709	1348.708	1262.611	818.953
579.511	578.923	943.000	1410.266
604.509	731.342	1039.992	1095.116
1087.894	871.072	880.193	574.391
720.860	807.823	900.985	1314.287
602.349	820.055	889.499	1147.267
485.551	469.265	829.675	1107.010

TABLE A-9. U-EASTWARD WIND, LATITUDE 72 DEGREES NORTH

PRESSURE LEVEL

30MB	65MB	110MB	190MB
1605.425	761.073	-58.928	-152.975
1347.832	741.148	104.106	131.987
1147.000	616.666	64.700	-440.378
1079.320	313.077	-452.921	-896.422
1230.762	326.967	-434.537	-716.778
1099.283	120.370	-462.383	-814.908
1142.875	193.634	-393.755	-872.742
1130.692	320.618	-122.402	-416.574
1421.728	761.826	388.278	100.184
1574.822	970.456	713.196	414.205
1724.456	1170.930	1030.285	814.607
1633.135	1302.544	1137.922	821.439
1514.207	1330.805	911.099	393.758
1492.449	1390.014	775.201	181.884
1302.508	1170.555	429.964	-84.752
1350.552	728.031	66.819	-421.633
1509.615	874.818	350.398	2.256
1956.993	890.180	246.606	51.702
2146.386	1043.232	226.199	-34.825
2775.758	1040.079	225.412	-56.270
3097.965	954.668	424.056	204.684
3048.129	1220.831	315.744	-42.711
3118.872	1321.332	663.302	814.739
3391.082	1690.296	597.677	210.350
3182.813	1497.202	593.408	79.692
3455.877	1590.055	430.381	-316.039
3446.335	1617.975	539.301	5.633
3193.051	1587.011	561.000	-42.511
2789.481	1727.510	909.234	360.391
2064.105	1480.986	956.719	461.486
1515.898	1240.948	953.335	635.386
1137.942	667.261	455.291	374.086
840.417	610.877	476.234	565.017
592.234	410.107	322.960	516.374
730.222	418.653	259.727	272.014
954.406	600.556	472.048	479.163
1242.230	694.505	281.600	48.526
1486.276	1154.915	871.673	838.561
1261.499	910.259	623.938	469.355
1696.564	1048.021	644.022	423.412
1479.862	909.683	383.200	-112.971
1506.591	811.700	460.677	-46.320
1449.292	683.054	-56.181	-757.967
1212.801	490.274	48.384	-227.042
1283.072	651.913	116.791	-158.751

TABLE A-10. COMPUTER PROGRAM FOR CALCULATION OF α-STATISTICS FROM 3-D GCM WIND DATA.

```
PRINT 2800
PRINT 600
PRINT 200, (SUMW48(J),J=1,4),(AVGW48(K),K=1,4)
PRINT 2850
PRINT 600
PRINT 200,(SUMWP48(J),J=1,4),(AVGWP48(J),J=1,4)
PRINT 3300
PRINT 600
PRINT 200,((ALP148(I,J),J=1,4),(ALP248(I,K),K=1,4),I=1,99)
PRINT 3500
PRINT 600
PRINT 200,(CNTA148(J),J=1,4),(CNTA248(K),K=1,4)
PRINT 3700
PRINT 600
PRINT 200,(SUMA148(J),J=1,4),(SUMA248(K),K=1,4)
PRINT 3900
PRINT 600
PRINT 200,(AVGA148(J),J=1,4),(AVGA248(K),K=1,4)
PRINT 4100
PRINT 600
PRINT 200,(SDEVA12(J),J=1,4),(SDEVA22(K),K=1,4)
PRINT 4300
PRINT 600
PRINT 200,((DEVA148(I,J),J=1,4),(DEVA248(I,K),K=1,4),I=1,99)
PRINT 4500
PRINT 600
PRINT 200,(AVGA12(J),J=1,4),(AVGA22(K),K=1,4)
PRINT 4700
PRINT 600
PRINT 200,(RG148(J),J=1,4),(RG248(K),K=1,4)
PRINT 2300
PRINT 600
PRINT 200, ((U72(I,J),J=1,4),(DEVU72(I,K),K=1,4),I=1,45)
PRINT 2400
PRINT 600
PRINT 200, ((V72(I,J),J=1,4),(DEVV72(I,K),K=1,4),I=1,45)
PRINT 2500
PRINT 600
PRINT 200, ((W72(I,J),J=1,4),(DEVW72(I,K),K=1,4),I=1,45)
PRINT 2900
PRINT 600
PRINT 200, (SUMU72(J),J=1,4),(AVGU72(K),K=1,4)
```

CONTINUED

TABLE 10 CONTINUED

```
      PRINT 3000
      PRINT 600
      PRINT 200, (SUMV72(J),J=1,4),(AVGV72(K),K=1,4)
      PRINT 3100
      PRINT 600
      PRINT 200, (SUMW72(J),J=1,4),(AVGW72(K),K=1,4)
      PRINT 3150
      PRINT 600
      PRINT 200,(SUMWP72(J),J=1,4),(AVGWP72(J),J=1,4)
      PRINT 3400
      PRINT 600
      PRINT 200,((ALP172(I,J),J=1,4),(ALP272(I,K),K=1,4),I=1,45)
      PRINT 3600
      PRINT 600
      PRINT 200,(CNTA172(J),J=1,4),(CNTA272(K),K=1,4)
      PRINT 3800
      PRINT 600
      PRINT 200,(SUMA172(J),J=1,4),(SUMA272(K),K=1,4)
      PRINT 4000
      PRINT 600
      PRINT 200,(AVGA172(J),J=1,4),(AVGA272(K),K=1,4)
      PRINT 4200
      PRINT 600
      PRINT 200,(SDEVA13(J),J=1,4),(SDEVA23(K),K=1,4)
      PRINT 4400
      PRINT 600
      PRINT 200,((DEVA172(I,J),J=1,4),(DEVA272(I,K),K=1,4),I=1,45)
      PRINT 4600
      PRINT 600
      PRINT 200,(AVGA13(J),J=1,4),(AVGA23(K),K=1,4)
      PRINT 4800
      PRINT 600
      PRINT 200,(RG172(J),J=1,4),(RG272(K),K=1,4)
  200 FORMAT(8F15.6)
  300 FORMAT(1H1,29X,*U24*,56X,*U24STAR*)
  400 FORMAT(1H1,29X,*V24*,56X,*V24STAR*)
  500 FORMAT(1H1,29X,*W24*,56X,*W24STAR*)
  600 FORMAT(2(9X,*3HMB*,11X,*65MB*,10X,*110MB*,10X,*190MB*),/)
  700 FORMAT(1H0,27X,*SUMU24*,55X,*AVGU24*)
  800 FORMAT(1H ,//,27X,*SUMV24*,55X,*AVGV24*)
  900 FORMAT(1H ,//,27X,*SUMW24*,55X,*AVGW24*)
  950 FORMAT(1H ,//,26X,*SUMWP24*,55X,*AVGWP24*)
 1200 FORMAT(1H1,27X,*ALP124*,55X,*ALP224*)
 1300 FORMAT(1H0,23X,*     POINTS TAKEN (A124)*,37X,*     POINTS TAKEN
     XA224)*)
```

TABLE 10 CONTINUED

```
1400 FORMAT(1H0,30X,*SUM OF A124*,43X,*SUM OF A224*)
1500 FORMAT(1H0,28X,*AVERAGE OF A124*,41X,*AVERAGE OF A224*)
1600 FORMAT(1H1,27X,*A124STAR*,54X,*A224STAR*)
1700 FORMAT(1H0,23X,*SUM OF A124STAR SQUARED*,37X,*SUM OF A224STAR SQUA
    XRED*)
1800 FORMAT(1H0,21X,*AVERAGE OF SUM OF A124STAR*,36X,*AVERAGE OF SUM OF
    X A224STAR*)
1900 FORMAT(1H0,27X,*RG124*,55X,*RG224*)
2000 FORMAT(1H1,29X,*U48*,56X,*U48STAR*)
2100 FORMAT(1H1,29X,*V48*,56X,*V48STAR*)
2200 FORMAT(1H1,29X,*W48*,56X,*W48STAR*)
2600 FORMAT(1H0,27X,*SUMU48*,55X,*AVGU48*)
2700 FORMAT(1H ,//,27X,*SUMV48*,55X,*AVGV48*)
2800 FORMAT(1H ,//,27X,*SUMW48*,55X,*AVGW48*)
2850 FORMAT(1H ,//,26X,*SUMWP48*,55X,*AVGWP48*)
3300 FORMAT(1H1,27X,*ALP148*,55X,*ALP248*)
3500 FORMAT(1H0,23X,*     POINTS TAKEN (A148)*,37X,*     POINTS TAKEN (
    XA248)*)
3700 FORMAT(1H0,30X,*SUM OF A148*,43X,*SUM OF A248*)
3900 FORMAT(1H0,28X,*AVERAGE OF A148*,41X,*AVERAGE OF A248*)
4300 FORMAT(1H1,27X,*A148STAR*,54X,*A248STAR*)
4100 FORMAT(1H0,23X,*SUM OF A148STAR SQUARED*,37X,*SUM OF A248STAR SQUA
    XRED*)
4500 FORMAT(1H0,21X,*AVERAGE OF SUM OF A148STAR*,36X,*AVERAGE OF SUM OF
    X A248STAR*)
4700 FORMAT(1H0,27X,*RG148*,55X,*RG248*)
2300 FORMAT(1H1,29X,*U72*,56X,*U72STAR*)
2400 FORMAT(1H1,29X,*V72*,56X,*V72STAR*)
2500 FORMAT(1H1,29X,*W72*,56X,*W72STAR*)
2900 FORMAT(1H0,27X,*SUMU72*,55X,*AVGU72*)
3000 FORMAT(1H ,//,27X,*SUMV72*,55X,*AVGV72*)
3100 FORMAT(1H ,//,27X,*SUMW72*,55X,*AVGW72*)
3150 FORMAT(1H ,//,26X,*SUMWP72*,55X,*AVGWP72*)
3400 FORMAT(1H1,27X,*ALP172*,55X,*ALP272*)
3600 FORMAT(1H0,23X,*     POINTS TAKEN (A172)*,37X,*     POINTS TAKEN (
    XA272)*)
3800 FORMAT(1H0,30X,*SUM OF A172*,43X,*SUM OF A272*)
4000 FORMAT(1H0,28X,*AVERAGE OF A172*,41X,*AVERAGE OF A272*)
4400 FORMAT(1H1,27X,*A172STAR*,54X,*A272STAR*)
4200 FORMAT(1H0,23X,*SUM OF A172STAR SQUARED*,37X,*SUM OF A272STAR SQUA
    XRED*)
4600 FORMAT(1H0,21X,*AVERAGE OF SUM OF A172STAR*,36X,*AVERAGE OF SUM OF
    X A272STAR*)
4800 FORMAT(1H0,27X,*RG172*,55X,*RG272*)
     STOP
```

TABLE 10 CONTINUED

```
  MFA    NOS/BF 1.3           IDA 488   05/23/79
11.16.16.ULIST2B  FROM
11.16.16.IP  00002304 WORDS - FILE INPUT  , DC 04
11.16.16.ULIST, 060.000,OPERATOR,J,0856
11.16.17.ILLEGAL USER NAME.
11.16.17.COPYSBF(INPUT,OUTPUT)
11.16.19.OP  00002304 WORDS - FILE OUTPUT , DC 40
11.16.19.MS     3584  WORDS  (    3584 MAX USED)
11.16.19.CPA        .113 SEC.          .112 ADJ.
11.16.19.IO         .239 SEC.          .239 ADJ.
11.16.19.CM        2.430 KWS.          .148 ADJ.
11.16.19.SS                            .499
11.16.19.PP        1.926 SEC.      DATE 11/29/79
11.16.19.EJ  END OF JOB, **

***********          ULIST2B  //// END OF LIST ////
***********          ULIST2B  //// END OF LIST ////
```

TABLE 10. CONTINUED

```
      PROGRAM FALL(INPUT,OUTPUT)
      DIMENSION U24(138,4),U48(99,4),U72(45,4),V24(138,4),V48(99,4),
     X          V72(45,4),W24(138,4),W48(99,4),W72(45,4),SUMU24(4),
     X          SUMU48(4),SUMU72(4),SUMV24(4),SUMV48(4),SUMV72(4),
     X          SUMW24(4),SUMW48(4),SUMW72(4),AVGU24(4),AVGU48(4),
     X          AVGU72(4),AVGV24(4),AVGV48(4),AVGV72(4),AVGW24(4),
     X          AVGW48(4),AVGW72(4),DEVU24(138,4),DEVU48(99,4),
     X          DEVU72(45,4),DEVV24(138,4),DEVV48(99,4),DEVV72(45,4),
     X          DEVW24(138,4),DEVW48(99,4),DEVW72(45,4),ALP124(138,4),
     X          ALP148(99,4),ALP172(45,4),ALP224(138,4),ALP248(99,4),
     X          ALP272(45,4),SUMA124(4),SUMA148(4),SUMA172(4),SUMA224(4)
     X          ,SUMA248(4),SUMA272(4),AVGA124(4),AVGA148(4),AVGA172(4),
     X          AVGA224(4),AVGA248(4),AVGA272(4),DEVA124(138,4),
     X          DEVA148(99,4),DEVA172(45,4),DEVA224(138,4),
     X          DEVA248(99,4),DEVA272(45,4),SDEVA11(4),SDEVA12(4),
     X          SDEVA13(4),SDEVA21(4),SDEVA22(4),SDEVA23(4),RG124(4),
     X          RG148(4),RG172(4),RG224(4),RG248(4),RG272(4),CNTA124(4),
     X          CNTA148(4),CNTA172(4),CNTA224(4),CNTA248(4),CNTA272(4),
     X          AVGA11(4),AVGA12(4),AVGA13(4),AVGA21(4),AVGA22(4),
     X          AVGA23(4)
      DIMENSION SAVEU24(138,4),SAVEV24(138,4),SAVEW24(138,4),SUMWP24(4),
     X          SUBW24(138,4),AVGWP24(4),DEVWP24(138,4),
     X          SAVEU48(99,4),SAVEV48(99,4),SAVEW48(99,4),SUMWP48(4),
     X          SUBW48(99,4),AVGWP48(4),DEVWP48(99,4),SAVEU72(45,4),
     X          SAVEV72(45,4),SAVEW72(45,4),SUMWP72(4),SUBW72(45,4),
     X          AVGWP72(4),DEVWP72(45,4)
C
C     CUTOFF IS THE VALUE (IN RADIANS) FOR WHICH ALPHA1
C         AND ALPHA2 CANNOT BE EQUAL TO OR GREATER THAN
C
      DATA CUTOFF/.34/
      DO 1 J=1,4
    1    READ 100,(U24(I,J),I=1,138)
      DO 2 J=1,4
    2    READ 100,(U48(I,J),I=1,99)
      DO 3 J=1,4
    3    READ 100,(U72(I,J),I=1,45)
      DO 4 J=1,4
    4    READ 100,(V24(I,J),I=1,138)
      DO 5 J=1,4
    5    READ 100,(V48(I,J),I=1,99)
      DO 6 J=1,4
    6    READ 100,(V72(I,J),I=1,45)
      DO 7 J=1,4
    7    READ 100,(W24(I,J),I=1,138)
```

TABLE 10. CONTINUED

```
      DO 8 J=1,4
 8       READ 100,(W48(I,J),I=1,99)
      DO 9 J=1,4
 9       READ 100,(W72(I,J),I=1,45)
 100  FORMAT(8F10.3)
C
C     XMIT TRANSFERS THE INITIAL NUMBER OF POINTS TO EACH ELEMENT OF THE
C          CNT ARRAYS ASSOCIATED WITH ALPHA1 AND ALPHA2 FOR THE
C          THREE DIFFERENT THETAS
C
      CALL XMIT(-4,138.,CNTA124)
      CALL XMIT(-4,138.,CNTA224)
      CALL XMIT(-4,99.,CNTA148)
      CALL XMIT(-4,99.,CNTA248)
      CALL XMIT(-4,45.,CNTA172)
      CALL XMIT(-4,45.,CNTA272)
 15   FLAG1=0.
      FLAG2=0.
      CALL XMIT(-4,0,SUMU24)
      CALL XMIT(-4,0,SUMV24)
      CALL XMIT(-4,0,SUMW24)
      CALL XMIT(-4,0,SUMWP24)
      DO 10 J=1,4
C
C      LOOPS 10 THROUGH 120 COMPUTE THE SUMS, AVERAGES, AND STARS
C          NEEDED TO COMPUTE THE REED-GERMANS FOR THETA=24 DEGREES
C
         DO 10 I=1,138
            SUMU24(J)=SUMU24(J)+U24(I,J)-SAVEU24(I,J)
            SUMV24(J)=SUMV24(J)+V24(I,J)-SAVEV24(I,J)
            SUMW24(J)=SUMW24(J)+W24(I,J)-SAVEW24(I,J)
            SUMWP24(J)=SUMWP24(J)+W24(I,J)-SUBW24(I,J)
 10   CONTINUE
      DO 20 J=1,4
         AVGU24(J)=SUMU24(J)/ CNTA224(J)
         AVGV24(J)=SUMV24(J)/CNTA124(J)
         AVGW24(J)=SUMW24(J)/CNTA124(J)
         AVGWP24(J)=SUMWP24(J)/CNTA224(J)
 20   CONTINUE
      DO 30 J=1,4
         DO 30 I=1,138
            IF(SAVEU24(I,J) .EQ. 0) DEVU24(I,J)=U24(I,J)-AVGU24(J)
            IF(SAVEV24(I,J) .EQ. 0) DEVV24(I,J)=V24(I,J)-AVGV24(J)
            IF(SAVEW24(I,J) .EQ. 0) DEVW24(I,J)=W24(I,J)-AVGW24(J)
            IF(SUBW24(I,J) .EQ. 0) DEVWP24(I,J)=W24(I,J)-AVGWP24(J)
 30   CONTINUE
```

TABLE 10. CONTINUED

```
      DO 40 J=1,4
C
C     LOOPS 40 AND 50 COMPUTE ALPHA1 AND ALPHA2, DROPPING THOSE
C           POINTS GREATER THAN CUTOFF
C
         DO 40 I=1,138
      IF(ALP124(I,J) .EQ. 3.15) GO TO 40
            ALP124(I,J)=ATAN(DEVW24(I,J)/DEVV24(I,J))
            IF(ABS(ALP124(I,J)) .LE. CUTOFF) GO TO 40
               SAVEW24(I,J)=W24(I,J)
               SAVEV24(I,J)=V24(I,J)
               ALP124(I,J)=3.15
               CNTA124(J)=CNTA124(J)-1.
               FLAG1=1.
 40   CONTINUE
      DO 50 J=1,4
         DO 50 I=1,138
      IF(ALP224(I,J) .EQ. 3.15) GO TO 50
            ALP224(I,J)=ATAN(DEVWP24(I,J)/DEVU24(I,J))
            IF(ABS(ALP224(I,J)) .LE. CUTOFF) GO TO 50
               SUBW24(I,J)=W24(I,J)
               SAVEU24(I,J)=U24(I,J)
               ALP224(I,J)=3.15
               CNTA224(J)=CNTA224(J)-1.
               FLAG2=1.
 50      CONTINUE
C
C     IF ANY POINTS HAVE BEEN DROPPED, RECOMPUTE
C
      IF(FLAG1 .EQ. 1 .OR. FLAG2 .EQ. 1) GO TO 15
      DO 60 J=1,4
         DO 60 I=1,138
      IF(ALP124(I,J) .EQ. 3.15) GO TO 65
               SUMA124(J)=SUMA124(J)+ALP124(I,J)
 65   IF(ALP224(I,J) .EQ. 3.15) GO TO 60
               SUMA224(J)=SUMA224(J)+ALP224(I,J)
 60   CONTINUE
      DO 70 J=1,4
         AVGA124(J)=SUMA124(J)/CNTA124(J)
         AVGA224(J)=SUMA224(J)/CNTA224(J)
 70   CONTINUE
      DO 80 J=1,4
         DO 80 I=1,138
            IF(ALP124(I,J) .EQ. 3.15) GO TO 85
               DEVA124(I,J)=ALP124(I,J)-AVGA124(J)
 85         IF(ALP224(I,J) .EQ. 3.15) GO TO 80
               DEVA224(I,J)=ALP224(I,J)-AVGA224(J)
 80   CONTINUE
```

TABLE 10. CONTINUED

```
      DO 90 J=1,4
         DO 90 I=1,138
            SDEVA11(J)=SDEVA11(J)+DEVA124(I,J)**2
            SDEVA21(J)=SDEVA21(J)+DEVA224(I,J)**2
 90   CONTINUE
      DO 110 J=1,4
         AVGA11(J)=SDEVA11(J)/CNTA124(J)
         AVGA21(J)=SDEVA21(J)/CNTA224(J)
110   CONTINUE
      DO 120 J=1,4
         RG124(J)=AVGA11(J)/AVGA124(J)**2
         RG224(J)=AVGA21(J)/AVGA224(J)**2
120   CONTINUE
125   FLAG1=0.
      FLAG2=0.
      CALL XMIT(-4,0,SUMU48)
      CALL XMIT(-4,0,SUMV48)
      CALL XMIT(-4,0,SUMW48)
      CALL XMIT(-4,0,SUMWP48)
C
C     LOOPS 130 THROUGH 240 COMPUTE THE SUMS, AVERAGES, AND STARS
C         NEEDED TO COMPUTE THE REED-GERMANS FOR THETA=48 DEGREES
C
      DO 130 J=1,4
         DO 130 I=1,99
            SUMU48(J)=SUMU48(J)+U48(I,J)-SAVEU48(I,J)
            SUMV48(J)=SUMV48(J)+V48(I,J)-SAVEV48(I,J)
            SUMW48(J)=SUMW48(J)+W48(I,J)-SAVEW48(I,J)
            SUMWP48(J)=SUMWP48(J)+W48(I,J)-SUBW48(I,J)
130   CONTINUE
      DO 140 J=1,4
         AVGU48(J)=SUMU48(J)/CNTA248(J)
         AVGV48(J)=SUMV48(J)/CNTA148(J)
         AVGW48(J)=SUMW48(J)/CNTA148(J)
         AVGWP48(J)=SUMWP48(J)/CNTA248(J)
140   CONTINUE
      DO 150 J=1,4
         DO 150 I=1,99
            IF(SAVEU48(I,J) .EQ. 0) DEVU48(I,J)=U48(I,J)-AVGU48(J)
            IF(SAVEV48(I,J) .EQ. 0) DEVV48(I,J)=V48(I,J)-AVGV48(J)
            IF(SAVEW48(I,J) .EQ. 0) DEVW48(I,J)=W48(I,J)-AVGW48(J)
            IF(SUBW48(I,J) .EQ. 0) DEVWP48(I,J)=W48(I,J)-AVGWP48(J)
150   CONTINUE
      DO 160 J=1,4
C
C     LOOPS 160 AND 170 COMPUTE ALPHA1 AND ALPHA2, DROPPING THOSE
C         POINTS GREATER THAN CUTOFF
C
```

TABLE 10. CONTINUED

```
         DO 160 I=1,99
      IF(ALP148(I,J) .EQ. 3.15) GO TO 160
            ALP148(I,J)=ATAN(DEVW48(I,J)/DEVV48(I,J))
            IF(ABS(ALP148(I,J)).LE. CUTOFF) GO TO 160
               SAVEW48(I,J)=W48(I,J)
               SAVEV48(I,J)=V48(I,J)
               ALP148(I,J)=3.15
               CNTA148(J)=CNTA148(J)-1.
               FLAG1=1.
 160  CONTINUE
      DO 170 J=1,4
         DO 170 I=1,99
      IF(ALP248(I,J) .EQ. 3.15) GO TO 170
            ALP248(I,J)=ATAN(DEVWP48(I,J)/DEVU48(I,J))
            IF(ABS(ALP248(I,J)).LE. CUTOFF) GO TO 170
               SUBW48(I,J)=W48(I,J)
               SAVEU48(I,J)=U48(I,J)
               ALP248(I,J)=3.15
               CNTA248(J)=CNTA248(J)-1.
               FLAG2=1.
 170  CONTINUE
C
C     IF ANY POINTS HAVE BEEN DROPPED, RECOMPUTE
C
      IF(FLAG1 .EQ. 1 .OR. FLAG2 .EQ. 1) GO TO 125
      DO 180 J=1,4
         DO 180 I=1,99
      IF(ALP148(I,J) .EQ. 3.15) GO TO 185
            SUMA148(J)=SUMA148(J)+ALP148(I,J)
 185  IF(ALP248(I,J) .EQ. 3.15) GO TO 180
            SUMA248(J)=SUMA248(J)+ALP248(I,J)
 180  CONTINUE
      DO 190 J=1,4
         AVGA148(J)=SUMA148(J)/CNTA148(J)
         AVGA248(J)=SUMA248(J)/CNTA248(J)
 190  CONTINUE
      DO 210 J=1,4
         DO 210 I=1,99
            IF(ALP148(I,J) .EQ. 3.15) GO TO 215
               DEVA148(I,J)=ALP148(I,J)-AVGA148(J)
 215        IF(ALP248(I,J) .EQ. 3.15) GO TO 210
               DEVA248(I,J)=ALP248(I,J)-AVGA248(J)
 210  CONTINUE
      DO 220 J=1,4
         DO 220 I=1,99
            SDEVA12(J)=SDEVA12(J)+DEVA148(I,J)**2
            SDEVA22(J)=SDEVA22(J)+DEVA248(I,J)**2
 220  CONTINUE
```

TABLE 10. CONTINUED

```
      DO 230 J=1,4
         AVGA12(J)=SDEVA12(J)/CNTA148(J)
         AVGA22(J)=SDEVA22(J)/CNTA248(J)
 230  CONTINUE
      DO 240 J=1,4
         RG148(J)=AVGA12(J)/AVGA148(J)**2
         RG248(J)=AVGA22(J)/AVGA248(J)**2
 240  CONTINUE
 255  FLAG1=0.
      FLAG2=0.
      CALL XMIT(-4,0,SUMU72)
      CALL XMIT(-4,0,SUMV72)
      CALL XMIT(-4,0,SUMW72)
      CALL XMIT(-4,0,SUMWP72)
C
C     LOOPS 250 THROUGH 360 COMPUTE THE SUMS, AVERAGES, AND STARS
C         NEEDED TO COMPUTE THE REED-GERMANS FOR THETA=72 DEGREES
C
      DO 250 J=1,4
         DO 250 I=1,45
            SUMU72(J)=SUMU72(J)+U72(I,J)-SAVEU72(I,J)
            SUMV72(J)=SUMV72(J)+V72(I,J)-SAVEV72(I,J)
            SUMW72(J)=SUMW72(J)+W72(I,J)-SAVEW72(I,J)
            SUMWP72(J)=SUMWP72(J)+W72(I,J)-SUPW72(I,J)
 250  CONTINUE
      DO 260 J=1,4
         DO 260 I=1,45
            AVGU72(J)=SUMU72(J)/CNTA272(J)
            AVGV72(J)=SUMV72(J)/CNTA172(J)
            AVGW72(J)=SUMW72(J)/CNTA172(J)
            AVGWP72(J)=SUMWP72(J)/CNTA272(J)
 260  CONTINUE
      DO 270 J=1,4
         DO 270 I=1,45
            IF(SAVEU72(I,J) .EQ. 0) DEVU72(I,J)=U72(I,J)-AVGU72(J)
            IF(SAVEV72(I,J) .EQ. 0) DEVV72(I,J)=V72(I,J)-AVGV72(J)
            IF(SAVEW72(I,J) .EQ. 0) DEVW72(I,J)=W72(I,J)-AVGW72(J)
            IF(SUPW72(I,J) .EQ. 0) DEVWP72(I,J)=W72(I,J)-AVGWP72(J)
 270  CONTINUE
C
C     LOOPS 280 AND 290 COMPUTE ALPHA1 AND ALPHA2, DROPPING THOSE
C       POINTS GREATER THAN CUTOFF
C
```

TABLE 10. CONTINUED

```
      DO 280 J=1,4
         DO 280 I=1,45
      IF(ALP172(I,J) .EG. 3.15) GO TO 280
            ALP172(I,J)=ATAN(DEVW72(I,J)/DEVV72(I,J))
            IF(ABS(ALP172(I,J)).LE. CUTOFF) GO TO 280
               SAVEW72(I,J)=W72(I,J)
               SAVEV72(I,J)=V72(I,J)
               ALP172(I,J)=3.15
               CNTA172(J)=CNTA172(J)-1.
               FLAG1=1.
 280  CONTINUE
      DO 290 J=1,4
         DO 290 I=1,45
      IF(ALP272(I,J) .EG. 3.15) GO TO 290
            ALP272(I,J)=ATAN(DEVWP72(I,J)/DEVU72(I,J))
            IF(ABS(ALP272(I,J)).LE. CUTOFF) GO TO 290
               SUBW72(I,J)=W72(I,J)
               SAVEU72(I,J)=U72(I,J)
               ALP272(I,J)=3.15
               CNTA272(J)=CNTA272(J)-1.
               FLAG2=1.
 290  CONTINUE
C
C     IF ANY POINTS HAVE BEEN DROPPED, RECOMPUTE
C
      IF(FLAG1 .EG. 1 .OR. FLAG2 .EQ. 1) GO TO 255
      DO 310 J=1,4
         DO 310 I=1,45
      IF(ALP172(I,J) .EG. 3.15) GO TO 315
            SUMA172(J)=SUMA172(J)+ALP172(I,J)
 315  IF(ALP272(I,J) .EG. 3.15) GO TO 310
            SUMA272(J)=SUMA272(J)+ALP272(I,J)
 310  CONTINUE
      DO 320 J=1,4
         AVGA172(J)=SUMA172(J)/CNTA172(J)
         AVGA272(J)=SUMA272(J)/CNTA272(J)
 320  CONTINUE
      DO 330 J=1,4
         DO 330 I=1,45
            IF(ALP172(I,J) .EG.3.15) GO TO 335
               DEVA172(I,J)=ALP172(I,J)-AVGA172(J)
 335        IF(ALP272(I,J) .EG. 3.15) GO TO 330
               DEVA272(I,J)=ALP272(I,J)-AVGA272(J)
 330        CONTINUE
      DO 340 J=1,4
         DO 340 I=1,45
            SDEVA13(J)=SDEVA13(J)+DEVA172(I,J)**2
            SDEVA23(J)=SDEVA23(J)+DEVA272(I,J)**2
 340  CONTINUE
```

```
      DO 350 J=1,4
         AVGA13(J)=SDEVA13(J)/CNTA172(J)
         AVGA23(J)=SDEVA23(J)/CNTA272(J)
350   CONTINUE
      DO 360 J=1,4
         RG172(J)=AVGA13(J)/AVGA172(J)**2
         RG272(J)=AVGA23(J)/AVGA272(J)**2
360   CONTINUE
      PRINT 300
      PRINT 600
      PRINT 200, ((U24(I,J),J=1,4),(DEVU24(I,K),K=1,4),I=1,138)
      PRINT 400
      PRINT 600
      PRINT 200, ((V24(I,J),J=1,4),(DEVV24(I,K),K=1,4),I=1,138)
      PRINT 500
      PRINT 600
      PRINT 200, ((W24(I,J),J=1,4),(DEVW24(I,K),K=1,4),I=1,138)
      PRINT  700
      PRINT 600
      PRINT 200, (SUMU24(J),J=1,4),(AVGU24(K),K=1,4)
      PRINT  800
      PRINT 600
      PRINT 200, (SUMV24(J),J=1,4),(AVGV24(K),K=1,4)
      PRINT  900
      PRINT 600
      PRINT 200, (SUMW24(J),J=1,4),(AVGW24(K),K=1,4)
      PRINT 950
      PRINT 600
      PRINT 200,(SUMWP24(J),J=1,4),(AVGWP24(J),J=1,4)
      PRINT 1200
      PRINT 600
      PRINT 200,((ALP124(I,J),J=1,4),(ALP224(I,K),K=1,4),I=1,138)
      PRINT 1300
      PRINT 600
      PRINT 200,(CNTA124(J),J=1,4),(CNTA224(K),K=1,4)
      PRINT 1400
      PRINT 600
      PRINT 200,(SUMA124(J),J=1,4),(SUMA224(K),K=1,4)
      PRINT 1500
      PRINT 600
      PRINT 200,(AVGA124(J),J=1,4),(AVGA224(K),K=1,4)
      PRINT 1700
      PRINT 600
      PRINT 200,(SDEVA11(J),J=1,4),(SDEVA21(K),K=1,4)
      PRINT 1600
      PRINT 600
      PRINT 200,((DEVA124(I,J),J=1,4),(DEVA224(I,K),K=1,4),I=1,138
```

TABLE 10. CONTINUED

```
PRINT 1800
PRINT 600
PRINT 200,(AVGA11(J),J=1,4),(AVGA21(K),K=1,4)
PRINT 1900
PRINT 600
PRINT 200,(RG124(J),J=1,4),(RG224(K),K=1,4)
PRINT 2000
PRINT 600
PRINT 200, ((U48(I,J),J=1,4),(DEVU48(I,K),K=1,4),I=1,99)
PRINT 2100
PRINT 600
PRINT 200, ((V48(I,J),J=1,4),(DEVV48(I,K),K=1,4),I=1,99)
PRINT 2200
PRINT 600
PRINT 200, ((W48(I,J),J=1,4),(DEVW48(I,K),K=1,4),I=1,99)
PRINT 2600
PRINT 600
PRINT 200, (SUMU48(J),J=1,4),(AVGU48(K),K=1,4)
PRINT 2700
PRINT 600
PRINT 200, (SUMV48(J),J=1,4),(AVGV48(K),K=1,4)
```

*U.S. GOVERNMENT PRINTING OFFICE : 1980 0-721-894/288

END

DATE
FILMED

1-81

DTIC